CENTER FOR INFRASTRUCTURE ENGINEERING STUDIES

Reinforced Concrete Beams Strengthened with CFRP Composites: Failure due to Concrete Cover Delamination

by

J. Gustavo Tumialan

Abdeljelil Belarbi

Antonio Nanni

Department of Civil Engineering

University of Missouri - Rolla

March 1999

CIES

99-01

Disclaimer

The contents of this report reflect the views of the author(s), who are responsible for the facts and the accuracy of information presented herein. This document is disseminated under the sponsorship of the Center for Infrastructure Engineering Studies (CIES), University of Missouri -Rolla, in the interest of information exchange. CIES assumes no liability for the contents or use thereof.

The mission of CIES is to provide leadership in research and education for solving society's problems affecting the nation's infrastructure systems. CIES is the primary conduit for communication among those on the UMR campus interested in infrastructure studies and provides coordination for collaborative efforts. CIES activities include interdisciplinary research and development with projects tailored to address needs of federal agencies, state agencies, and private industry as well as technology transfer and continuing/distance education to the engineering community and industry.

Center for Infrastructure Engineering Studies (CIES)
University of Missouri-Rolla
223 Engineering Research Laboratory
1870 Miner Circle

Rolla, MO 65409-070
Tel: (573) 341-6223; fax -6215
E-mail: cies@umr.edu
www.cies.umr.edu

Reinforced Concrete Beams Strengthened with CFRP Composites: Failure due to Concrete Cover Delamination

by

J. Gustavo Tumialan

Abdeljelil Belarbi

Antonio Nanni

Department of Civil Engineering

University of Missouri - Rolla

Report No. CIES 99-01

Center for Infrastructure Engineering Studies

University of Missouri - Rolla

ABSTRACT

In addition to the conventional modes of failure observed in RC beams, some premature modes of failure can be observed in beams strengthened by means of externally bonded plates or sheets such as concrete cover delamination or peeling-off of the CFRP sheet. This kind of failure is caused by shear transfer mechanisms and local regions of tension at the interface between the concrete and CFRP.

A series of tests was carried out in order to study the concrete cover delamination failure, wherein the variables were length of beam span, bonded area, number of plies, and U-jacketing schemes. Two failure mechanisms within the concrete cover delamination were observed. One was caused by cover delamination at the cutoff point of the sheets, Failure Mode I, which was originated by a high concentration of normal (out-of-plane) and shear stresses. A second one, called Failure Mode II, caused by cover delamination starting from an intermediate flexural crack between the outermost crack and the maximum bending area. The latter mode of failure was originated by splitting of concrete at the steel reinforcement level, and, mainly, by normal and shear stresses at the level of the steel reinforcement. The use of U-jackets is shown to lessen the effect of cover delamination. The mechanisms of the observed modes of failure are described. For Failure Mode I, an analytical approach to estimate the shear and normal stresses at the curtailment of FRP sheets is presented. The mechanism of Failure Mode II is complex. Schemes intending to predict the failure are presented. They can include the analysis of an element between two flexural cracks and the assumption of certain normal stress distribution similar to that employed for Mode I. This may serve as framework for future investigations.

ACKNOWLEDGMENTS

The authors would like to acknowledge the financial support of the Mid-America Transportation Center (MATC), headquartered on the University of Nebraska, and Mitsubishi Chemical Corporation of Tokyo, Japan.

TABLE OF CONTENTS

APPENDICES

LIST OF ILLUSTRATIONS

LIST OF TABLES

LIST OF ABBREVIATIONS AND SYMBOLS

Ef = modulus of elasticity of FRP sheets

Ec = modulus of elasticity of concrete

Ga = shear modulus of adhesive

$\bar{h}$ = neutral axis for uncracked section (measured from the bottom)

I = moment of Inertia of the uncracked section transformed to concrete

M = moment at the end of the FRP sheets

tf = thickness of FRP sheets

ta = thickness of adhesive

V = shear force at the end of the FRP sheets

wf = width of the FRP sheet

σ_x = stress in the x-direction

σ_y = stress in the y-direction

τ = shear stress

σ_p = maximum principal stress

θ_p = orientation of the principal plane

μ = ductility

δu = deflection at the ultimate state of failure

δy = deflection at the yielding of steel

1. INTRODUCTION

1.1. BACKGROUND

Strengthening of Reinforced Concrete (RC) structures by bonding external steel and composites plates or sheets is an effective method for improving structural performance under both service and ultimate load conditions. Also, it has been shown that plate or sheet bonding reduces crack widths and deflections (Chaallal, Nollet, Saleh, 1998). A main disadvantage of using steel plates is the corrosion that occurs when plates are exposed to harsh environments. Other disadvantages are transportation, storage, installation difficulties, as well as the addition of self-weight to the structure. On the other hand, the employment of composite sheets offers several advantages such as ease of bonding to curved or irregular surfaces, lightweight, and the fact that fibers can be oriented along the direction.

Applications of composite materials are found in many industries such as automotive, aviation and aerospace, biomedical industries and leisure. The introduction of composite materials to the Civil Infrastructure is a relatively new technology; but, it has increased dramatically in the last few years. In this context, externally bonded Carbon Fiber Reinforced Polymer (CFRP) sheets are one of the most promising uses.

CFRP sheets provide solutions for strengthening beams, slabs, walls, columns, and other structural elements that are subjected to deterioration, additional service loads, or excessive deflections created by change in use, construction or design defects, code changes or retrofit.

1.2. SCOPE AND OBJECTIVES

The failure of a RC member strengthened in flexure can be caused by the crushing of concrete, rupture of the CFRP laminate, peeling-off, or concrete cover delamination. In the first two modes of failure, the ultimate strength of the structural member can be easily predicted by following conventional RC flexural theory. However, whenever the mode of failure is peeling-off or concrete cover delamination, the strengthened member is not able to reach its ultimate strength; hence, the prediction of these kinds of failures is not an easy task. These failures are sudden, brittle, and without warning. Terms such as peeling-off or ripping-off have been used in previous studies to describe cover delamination as well (Roberts, 1989). Although it is clear that the term used is unimportant but to understand the concept, the mechanism and the prevention of this mode of failure, the term "concrete cover delamination" is proposed in order to differentiate it from peeling-off.

The use of this term is reasonable. It has been observed that the horizontal shear crack found in this kind of failure occurs at a distance equal to the effective concrete cover of the longitudinal steel reinforcement from the extreme tension face of the beam. This mode of failure is different from the so-called peeling-off failure, where the externally bonded reinforcement is partially peeled from the concrete surface.

This concrete cover delamination failure is caused by shear and local regions of tension (out-of-plane) stresses at the level of the steel reinforcement. The magnitude of these stresses that may develop prior to failure is influenced by material properties such as tensile and shear strength of the concrete and modulus of elasticity of the plate and the adhesive. Also, it is influenced by geometrical parameters such as thickness of the external reinforcement and adhesive, and distance of the end of the plates or sheets from the support.

As part of this study, RC beams strengthened with CFRP sheets were tested and evaluated. Variables such as the number of plies of CFRP, bonded area, span length, contribution of U-jacketing (wrapping), and stirrups spacing were studied. The test observations made it possible to distinguish two mechanisms within the cover delamination failure.

One failure mechanism was caused by cover delamination at the cutoff point of the sheets, which is originated by a high concentration of normal (out-of-plane) and shear stresses. The second failure mechanism was caused by cover delamination starting at an intermediate flexural crack between the outermost crack and the maximum bending area. The latter failure was originated by splitting the concrete at the steel reinforcement level, and mainly, by normal and shear stresses at that level.

Several analytical studies (Roberts, 1989; Malek, Saadatmanesh, Ehsani, 1998) have been conducted to predict and describe the behavior of structural members up to peeling-off or cover delamination failure. Although these research studies show acceptable values compared to experimental ones, they are difficult to use for design purposes because of the complexity of their equations. In addition, these models have been developed for plate bonding systems and not for sheet bonding systems. Therefore, the main objective of this thesis, from the analytical point of view, is to obtain a better understanding of the concrete cover delamination failure as well as implement schemes to predict it.

1.3. LAYOUT OF THE REPORT

This report is organized as follows:

Section 2 deals with a brief description of previous experimental and analytical studies on concrete cover delamination in beams strengthened with steel plates as well as composite plates and sheets. Two analytical models to predict the concentration of normal and shear stresses at the cutoff point are described, one for steel plates and the other for composite plates.

Section 3 deals with the description of the experimental program carried out at the Engineering Research Laboratory at UMR. The specimens tested in this research are described, as well as, the material constituents. A brief description of the test setup and the test itself is given.

Section 4 discussions on the test results are presented. The discussions on the test results are based on comparisons between the analytical and experimental curves, effects of the external reinforcement on stiffness and ductility, and the observations during the tests. A model to predict the load versus deflection response is developed.

Section 5 describes the analytical approach adopted in this report based on a previous analytical model for plates which is modified for sheets. The assumptions adopted in order to predict the behavior of the specimens are explained. In addition, the different situations in which the cover delamination failure is present are described.

Finally, Section 6 provides the concluding remarks and recommendations for future work.

2. LITERATURE REVIEW

2.1. STRENGTHENING WITH STEEL PLATES

Research on steel plates was conducted when L'Hermite and Bresson (1967) studied RC members strengthened by steel plates. Experimental works continued for the next ten years until this technique became an accepted field practice. Some of these studies are described in the following paragraphs.

Jones (1980) studied the behavior of plain and RC beams strengthened with epoxy bonded steel plates to their tension faces. The variables taken into account were the adhesive thickness, the plate lapping, the number of plates and the pre-cracking of the specimen prior to bonding. It was concluded that strengthening with steel plates increases the range of elastic behavior, reduces the tensile strain in the concrete due to the composite action, delays the appearance of the first visible cracks, and increases flexural stiffness.

Oehlers (1992) studied the premature failure of externally plated reinforced concrete beams. The geometry and material properties of the beams were varied, and the RC beams were subjected to pre-cracking. It was observed that shear diagonal cracks hastened separation of the plates from RC members, and flexural forces caused gradual separation. A method to determine the moment related to the cover delamination failure was derived. This failure was dependent on the flexural rigidity, tensile strength of the concrete, and the thickness of the plate.

On the analytical side, Roberts and co-workers (1989) conducted the most important work, which has been used for the derivation of several analytical studies. This study developed a model for predicting the effect of steel plates on the distribution of shear and normal stresses in the interface of the RC beam and the steel plate.

2.2. STRENGTHENING WITH COMPOSITE SYSTEMS

There are two composite systems to strengthen RC members: Plate Bonding (cured plates) and Sheet Bonding (wet lay-up). The main difference in the two composite systems is that in the Sheet Bonding, the impregnating resin is added in the field rather than during its manufacture. In this way, more than one sheet or ply can be bonded through the manual lay-up technique. Another difference is the order of magnitude in the thickness of the strengthening system. In the plate bonding system with composite plates, 0.05 in. is the average. In contrast, in the sheet bonding system the thickness is notoriously less. In this research, the thickness of the carbon fiber sheets was 0.0065 in.

2.2.1. FRP Plate Bonding. Saadatmanesh and Ehsani (1991) studied RC beams strengthened by glass fiber reinforced plastic (GRFP) plates to their tension faces. Some important conclusions were drawn from this research; for instance, the gain in the ultimate strength was more significant in beams with a lower steel reinforcement ratio. Also, the presence of the plates reduced the crack size in the beams; however, the ductility was reduced.

Sharif (1994) investigated the repair of initially loaded RC beams with epoxy-bonded glass FRP plates. In the first stage, the beams were loaded to 85% of the ultimate flexural capacity. In the second stage the beams were repaired with FRP plates bonded to the soffit of the beams. Different repair and anchoring schemes were conducted in order to avoid premature failures and to ensure ductile behavior. It was observed that the ductile behavior of the repaired beam was inversely proportional to the plate thickness. Also, it was concluded that the employment of I-jacket plates provided a good anchorage and improved the ductility of beams repaired with plates of large thicknesses.

Arduini and Di Tommaso (1995) conducted three point bending tests for plated concrete medium size beams as well as numerical simulations. Two different externally bonded reinforcements were used made up either of aramid fibers (AFRP) or glass fibers (GRFP). The results of this research showed that plate bonding considerably increases the load bearing capacity of the flexural member; and, furthermore the behavior of the specimen can be modified by the plate size, FRP and adhesive type, shear reinforcement and surfaces preparation. It was also observed that thicker plates led to cover delamination failure, which can be prevented or delayed by gluing plates to the lateral faces.

He, Pilakoutas and Waldron (1997) performed tests investigating the behavior of RC beams strengthened with CFRP plates. The results showed that the flexural capacity can be increased by bonding composite plates; even though, the chances of premature failure due to cover delamination increased. It was observed that beams strengthened with CFRP plates controlled cracks and deflections, and that the cover delamination failure was facilitated by shear cracking.

From the analytical standpoint, Kaiser (1989) showed the validity of the strain compatibility method, a classical approach for RC sections, in the analysis of repaired members. Wei An (1990) presented analytical models, which were based on the compatibility of deformations and equilibrium of forces, using the assumption that concrete carries no tension.

2.2.2. FRP Sheet Bonding. Chajes (1995) tested RC beams to study the ability of externally bonded composite reinforcement to improve their flexural and shear capacities. In order to study the effect of the CFRP sheets, variables such as the number of layers and the fiber orientation were taken in account. The test results showed that the composite reinforcement increased the flexural stiffness between 103 and 178 percent, as well as the ultimate capacity between 158 and 292 percent. The final failure of the beams were initiated either by tensile failure of the CFRP sheets or by shear failure of concrete. The tests showed a logical progression of failure modes from flexure to shear when the number of layers of CFRP was added, and a decrease in ductility. By wrapping the beam with a single CFRP sheet, shear failure was prevented but lead to a flexural failure, which started with tensile failure of the composite reinforcement.

M'Bazaa (1996) tested RC beams strengthened with CFRP sheets. The objectives of this investigation were to study the length and orientation of the externally bonded reinforcement in order to increase the flexural strength and the ductility. Also, this investigation was intended to evaluate the shear stress at the interface between the laminae and concrete and the anchorage length of the laminae. In order to do the above mentioned, the studied variables were the length and orientations ($+\theta^o$, $-\theta^o$, 0^o) of the laminae. This research confirmed that the externally bonded reinforcement increases the flexural strength, the stiffness, and the load under which the yield occurs. In this particular study, the use of symmetrical off-axis laminae with small angles from the longitudinal direction, and the employment of shortened CFRP sheets had no influence on the stiffness and ultimate strength.

Takahashi, Sato and Ueda (1997) obtained and compared experimental data on strength, stiffness and mode of failures of beams wrapped in U-jacket with CFRP sheets added to those not strengthened. This study showed that wrapping with U-jacket controls the cover delamination because the mode of failure can be changed from cover delamination to CFRP rupture. By wrapping the beam, the flexural strength was increased slightly; however, the deflection increased by about 50%.

Chaallal (1998) carried out the tests of RC beams strengthened in flexure and in shear using CFRP sheets. Some of the conclusions drawn were that strengthening beams in flexure showed more closely spaced, finer and more uniformly distributed cracks; and cover delamination caused the beam fails prematurely.

2.3. PREVIOUS ANALYTICAL WORK FOR STRESSES ON PLATES

Some analytical models have been developed to predict shear and normal stress concentrations at the plate end. These analyses are limited to the elastic range. In addition, the cover delamination failure is observed at the cutoff point of the plate when it is well known that this kind of failure can originate at any flexural crack location. In addition, the studied models have been developed for bonded plates where the thickness of the adhesive is relatively large compared to that in bonded sheets. In the sheet bonding system, this parameter is considerably smaller; in consequence, it is difficult to estimate in practice. Therefore, for design purposes, the value associated to the thickness of the adhesive should be limited to manufacturer's recommendations, field and laboratory samples, and analytical studies.

By understanding that this part of the thesis corresponds to the review of some of the available literature, a brief description of the studied models is given along with their assumptions and limitations. Further details are given in Section 5, wherein, the models are evaluated and compared to test results.

2.3.1 Roberts Analytical Model. Roberts conducted a three part analysis in order to predict the shear and normal stresses in the adhesive layer of RC beams strengthened with steel plates, as shown in Figure 2.1.

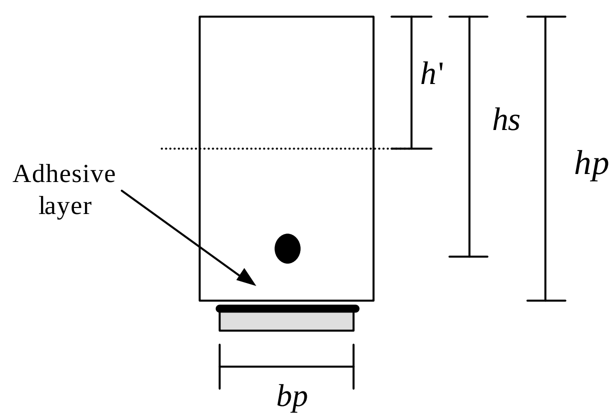

Figure 2.1. Cross Section Dimensions (Roberts Model)

In the first part, fully composite action between concrete and plate was assumed. Due to the applied loads, moment M and shear force V, a differential element in the plate, is under an axial force t_1, and a shear force by unit length

$\overline{t}_1$ in the adhesive, as shown in Figure 2.2. They can be determined by conventional mechanic of materials theory as follows:

$$\overline{t}_1 = \frac{V\,bp\,tp}{Is}(hp - h') \quad (1)$$

$$t_1 = \frac{Mbptp}{Is}(hp - h') \quad (2)$$

Where:

Is = Moment of inertia of the transformed equivalent steel section about the neutral axis.

h' = Depth of the neutral axis.

tp = Thickness of the plate

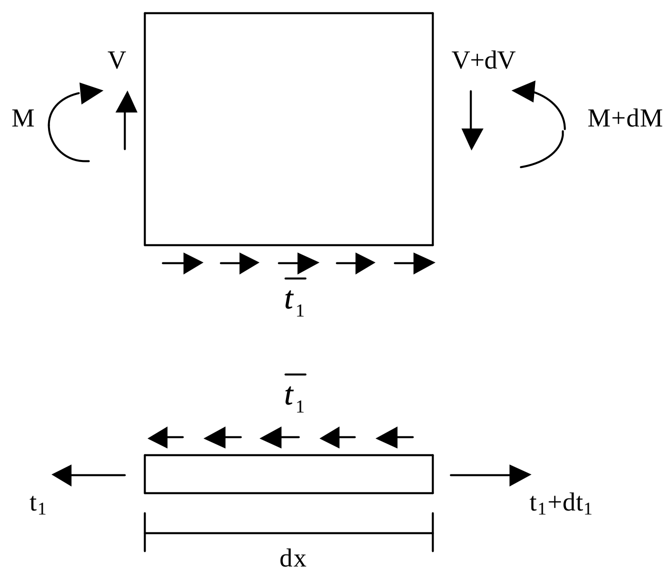

Figure 2.2. Resultant forces in a RC Beam Strengthened With Plates

In the second part of the solution two opposite forces, $-t_{10}$ and $-t_{1a}$, at the ends of the plate are applied because in fact they do not exist, as shown in Figure

2.3. In this part of the analysis, it is assumed that the plate is bonded to a rigid RC beam by an adhesive which has a shear stiffness by unit length Ks.

$$Ks = Ga\frac{ba}{ta} \tag{3}$$

Where:

Ga = shear modulus of the adhesive

ba = width of the adhesive

ta = thickness of the adhesive

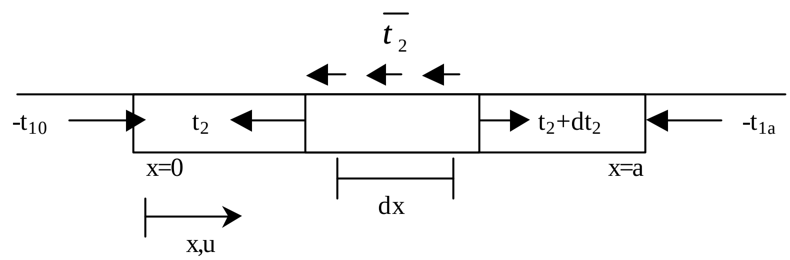

Figure 2.3. Forces in the Plate in Stage 2 of Analysis

By considering:

$$\overline{t}_2 = Ks\,u \tag{4}$$

$$t_2 = Ep\,bp\,tp\frac{du}{dx} \tag{5}$$

Where u is the displacement of the plate in the longitudinal axis, and E_p is the modulus of elasticity of the plate.

The governing differential equation is given by:

$$\frac{d^2u}{dx^2} - a^2 = 0 \tag{6}$$

$$a^2 = \frac{Ks}{Ep\,bp\,tp} \tag{7}$$

The shear force by unit length at the cutoff point when the second part is ended can be determined as:

$$\overline{t}_2 = \left(\frac{Ks}{Ep\,bp\,tp}\right)^{1/2} \left[\frac{M\,bp\,tp}{Is}\right](hp - h') \tag{8}$$

The resultant forces at the end of the second part are shown in Figure 2.4.

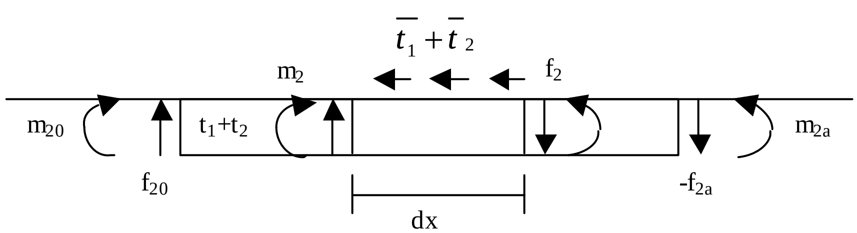

Figure 2.4. Forces in the Plate at the End of Stage 2

In the third part of the analysis, since the moments m_{20} and m_{2a} and forces f_{20} and f_{2a} at the ends of the plate do not exist, moments and forces are applied in the opposite direction, as shown in Figure 2.5. It is assumed that the plate is bonded to a rigid RC beam by an adhesive with normal stiffness by unit length Kn.

$$Kn = Ea\frac{ba}{ta} \tag{9}$$

where, Ea is the modulus of elasticity of the adhesive.

$$\overline{s_3} = Knw \tag{10}$$

w is the relative displacement of the plate in the transversal direction.

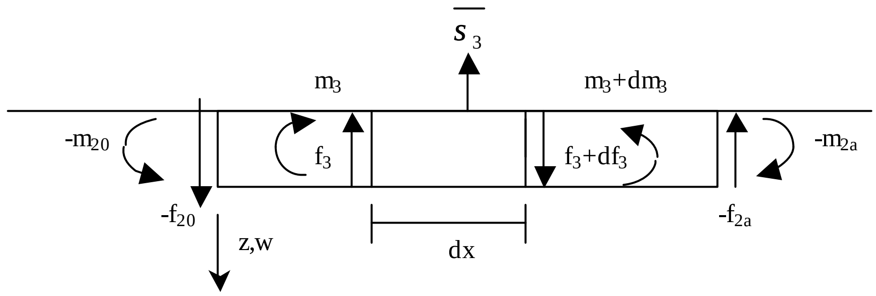

Figure 2.5. Forces in the Plate in Stage 3 of Analysis

Finally, the complete solution is obtained by superposition:

$$\overline{t} = \overline{t_1} + \overline{t_2} \tag{11}$$

$$\overline{s} = \overline{s_3} \tag{12}$$

In order to obtain the shear and normal stresses at the cutoff point of the plate, they are divided by the width of the plate, as follow:

$$t = \frac{t'}{bp} \tag{13}$$

$$s = \frac{s'}{bp} \tag{14}$$

The maximum shear and normal stresses at the above mentioned point are:

$$t_o = \left[V_o + \left(\frac{Ks}{Ep\,bp\,tp}\right)^{1/2} M_o\right]\frac{bp\,tp}{Is\,ba}(hp - h') \tag{15}$$

$$s_o = t_o\,tp\left(\frac{Kn}{4EpIp}\right)^{1/4} \tag{16}$$

where, V_o and M_o are the shear force and moment at the cutoff point of the plate.

2.3.2. Malek Analytical Model. This method was developed based on uncracked sections. The following assumptions are taken into account: linear elastic and isotropic behavior for FRP plates, adhesive, concrete and steel rebars; fully composite action between the plate and the concrete (no slip), and, linear strain distribution through the full depth of the section.

In order to predict the shear stress between the FRP plate and the adhesive layer the equilibrium of the infinitesimal part of the plate shown in Figure 2.6 is analyzed.

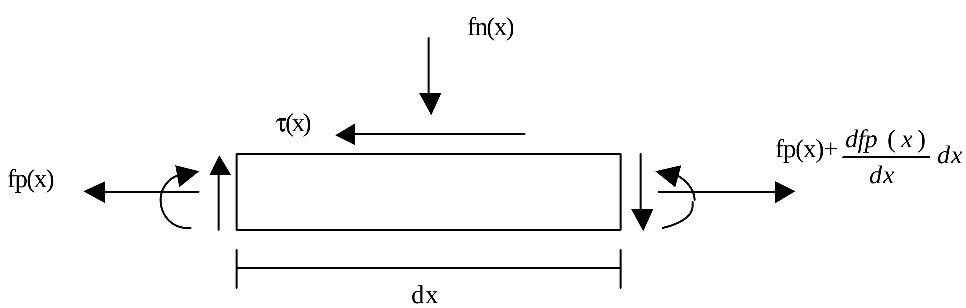

Figure 2.6. Stresses Acting on the Plate (Malek Model)

Where:

fp(x)= Tensile stress in the plate

t_p = Thickness of the plate

The shear stress is expressed as:

$$t(x) = \frac{dfp(x)}{dx} tp \tag{17}$$

Owing to the linear elastic behavior, the last equation can be expressed as:

$$\frac{dfp(x)}{dx} = \frac{Ga}{tp}\left(\frac{du}{dy} + \frac{dv}{dx}\right) \tag{18}$$

where:

Ga = shear modulus of elasticity of the adhesive layer

tp = thickness of the plate

u = horizontal displacement in the adhesive

v = vertical displacement in the adhesive

The relationship between the bending moment M and the deflection v is given by:

$$\frac{d^2v}{dx^2} = \frac{M}{Ec\,I} \tag{19}$$

By considering:

$$\frac{d^2u}{dxdy} = \frac{1}{ta}(e_p - e_c) \tag{20}$$

where:

Ec = modulus of elasticity of the concrete

I = moment of inertia of the transformed section to concrete

ε_p = interfacial strains in the lower face of the adhesive layer

ε_c = interfacial strains in the upper face of the adhesive layer

ta = thickness of the adhesive

By resolving the differential equations (17) and (18), it is possible to find fp(x) and τ(x). The complete solution can be referred from the original paper. The final equations for τ(x) is the following:

$$t\,(x) = tp\left[b_3\sqrt{A}\cosh(\sqrt{A}x) - b_3\sqrt{A}\sinh(\sqrt{A}x) + 2b_1x + b_2\right] \tag{21}$$

To develop equation (21), the origin *x* was assumed at the cutoff point of the plate.

$$A = \frac{Ga}{tatp\,Ep} \tag{22}$$

$$b_1 = \frac{\overline{y}\,a_1\,Ep}{I\,Ec} \tag{23}$$

$$b_2 = \frac{\overline{y}Ep}{IEc}(2a_1L_0 + a_2) \tag{24}$$

$$b_3 = Ep\left[\frac{\overline{y}}{I\,Ec}(a_1L_0^{\;2} + a_2L_0 + a_3) + 2b_1\frac{tatp}{Ga}\right] \tag{25}$$

The bending moment can be expressed as:

$$M(x_0) = a_1x_x^{\;2} + a_2x_o + a_3 \tag{26}$$

where the origin x_0 is arbitrary, and can be located at a distance L_0 from the cutoff point, this means, $x_0 = x + L_0$. The variable $\overline{y}$ represents the distance from the neutral axis of the cross section of the RC beam to the center of the FRP plate. The maximum shear stress found at the cutoff point is:

$$t_{\max} = tp(b_3\sqrt{A} + b_2) \tag{27}$$

In order to calculate the normal stress in the adhesive the FRP plate and the concrete are considered as two different beams connected by the adhesive layer as shown in Figure 2.7.

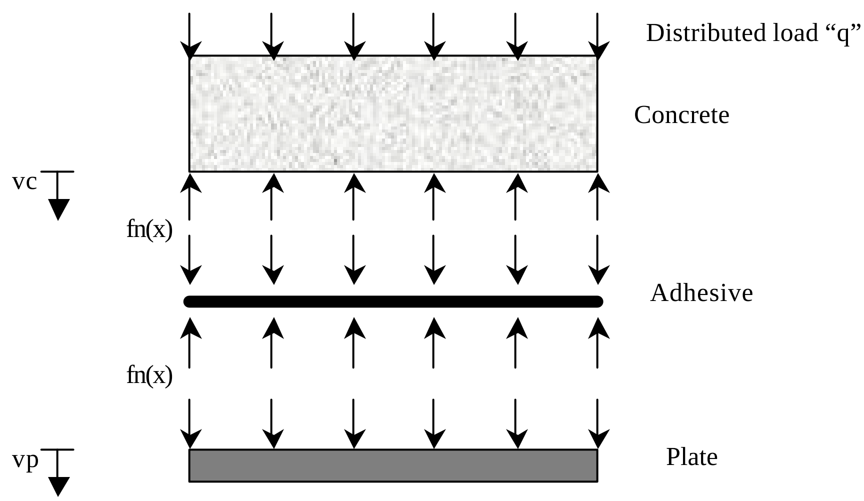

Figure 2.7. Normal Stresses Acting on Concrete and Plate

The normal stress *fn(x)* in the adhesive layer is:

$$fn(x) = Kn(v_p - v_c) \tag{28}$$

$$Kn = \frac{Ea}{ta} \tag{29}$$

where:

Ea = modulus of elasticity

ta = thickness of the adhesive

The normal stress *fn(x)* is obtained after resolving the following differential equations:

$$- Ec\,Ic \frac{d^4 v_c}{dx^4} = q - bp\ fn(x) \tag{30}$$

$$- Ep\,Ip \frac{d^4 v_p}{dx^4} = bp\ fn(x) \tag{31}$$

Where:

v_p = deflection of the FRP plate

v_c = deflection of the concrete beam

Ic = moment of Inertia of the FRP concrete

Ip = moment of Inertia of the FRP plate

bp = width of the FRP plate

q = distributed load on the concrete beam

The details of the complete solution are presented in the respective document. The final expressions are:

$$fn(x) = e^{-bx}\left[D_1 \cos(bx) + D_2 \sin(\ bx)\right] + \frac{q\,Ep\,Ip}{bp\,Ec\,Ic} \tag{32}$$

where:

$$D_1 = \frac{Kn}{EpIp} \cdot \frac{Vp}{2b^3} - \frac{Kn}{EcIc} \cdot \frac{Vc + bMo}{2b^3} \tag{33}$$

$$D_2 = \frac{Kn}{EcIc} \cdot \frac{Mo}{2b^2} \tag{34}$$

The bending moments in concrete and FRP plate are:

$$Mc = Mo \tag{35}$$

$$Mp = 0 \tag{36}$$

where, Mo is the bending moment in the concrete beam due to external loads.

The shear forces at the plate end in the concrete and FRP plate are:

$$Vc^{s} = -bp\,\overline{y_c}\,tpt_{\max} \tag{37}$$

$$Vp^{s} = -\frac{1}{2}bptp^{2}t_{\max} \tag{38}$$

The total shear force in the concrete beam and the FRP plate are:

$$Vc = Vo + Vc^{s} \tag{39}$$

$$Vp = Vp^{s} \tag{40}$$

where, Vo is the shear force in the concrete beam due to external loads.

The maximum normal stress, which occurs at the cutoff point, is expressed as:

$$fn_{\max} = \frac{Kn}{2\boldsymbol{b}^{3}}\left(\frac{Vp}{Ep\,Ip} - \frac{Vc + \boldsymbol{b}\,Mo}{Ec\,Ic}\right) + \frac{q\,Ep\,Ip}{bp\,Ec\,Ic} \tag{41}$$

2.3.3. Evaluation of the Analytical Models. In summary, the following assumptions were taken into account in the development of the Roberts and Malek Model:

- Linear elastic and isotropic behavior through the entire depth of the section.
- Fully composite action between FRP and concrete.

The cross section of a RC beam strengthened with 3 plies of CFRP, shown in Figure 2.8, is used to evaluate the Roberts and Malek Model.

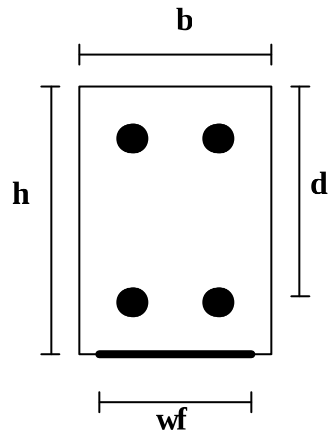

Figure 2.8. Geometry of the Analyzed Cross Section

- **Geometric properties**

  b = 6 in

  h = 12 in

  d = 10 in

  As = 0.62 in^2

  As’ = 0.62 in^2

  wf = 6 in

  thickness of sheet = 0.0065 in

- **Material properties**

  CFRP sheets

  Ef = 33400 Ksi

  Ea = 290 Ksi

  ? = 0.36

  Ga = 107 Ksi

Steel

fy = 62 Ksi

Es = 28300 Ksi

Concrete

f ‘c = 7500 psi

Ec = $57\sqrt{f'c} = 4936$ Ksi

The justifications of the assumptions taken into account to estimate the variables employed in the analytical models are given in Section 5.

Even though the Roberts Model was developed for steel plates and the Malek Model was developed for FRP plates, both obtained the same results, as can be verified in equations (42) and (43). Figure 2.9 shows the stress distributions for normal and shear stresses, and Figure 2.10 shows a magnification of the normal stress distribution (out-of-plane). A complete numerical evaluation of both models is given in Appendix D.

Normal Stress Distribution

$$\sigma(x) = e^{-x3.556}\left[-0.257\cos(3.556x) + 0.006\sin(3.556x)\right] \tag{42}$$

Peak value: $\sigma_{\max} = 0.257\ ksi$

Shear Stress Distribution

$$\tau(x) = 0.381\cosh(0.618x) - 0.381\sinh(0.618x) + 0.124 \tag{43}$$

Peak value: $\tau_{\max} = 0.505\ ksi$

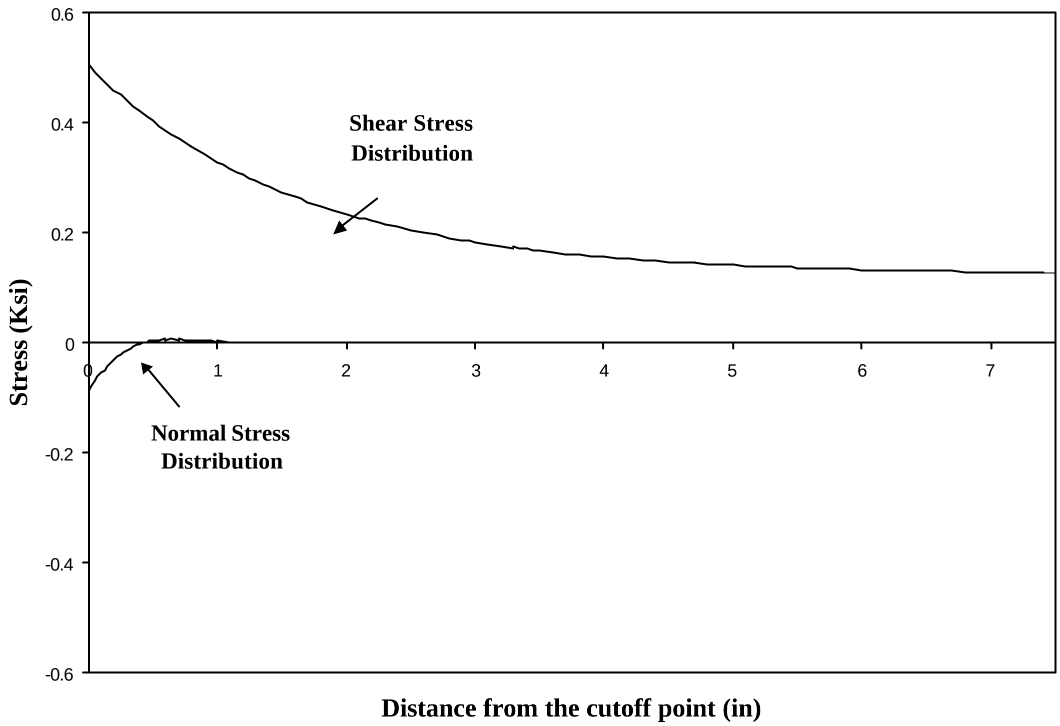

Figure 2.9. Normal and Shear Stress Distributions

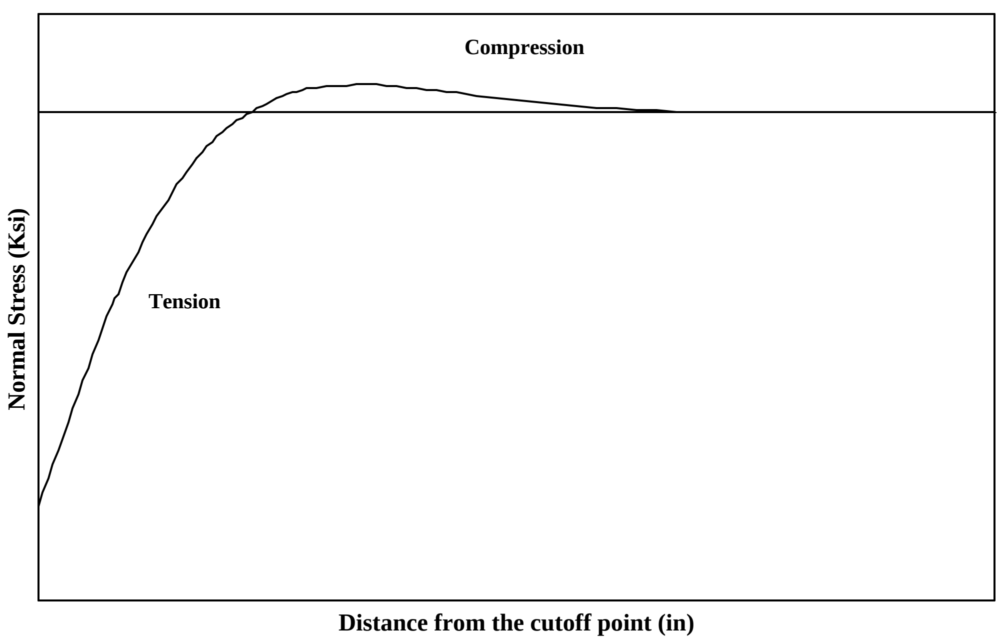

Figure 2.10. Normal Stress Distribution

The fact that the results are identical is logical due to the elastic analysis carried out in both studies. According to the Kirchoff's law, for each elastic equilibrium problem there is one and only one solution. The linear elastic behavior is justified by the fact that the cutoff points are usually located near the inflection or zero moments points wherein the normal stresses caused by the bending moments are low.

3. EXPERIMENTAL PROGRAM

3.1. DESCRIPTION OF RC BEAMS

A total of 16 RC beams with a rectangular cross section of 6 by 12 in. and length 14 ft were built for this experimental program. These beams were designed according to the requirements of the ACI 318-95. Figure 3.1 shows the cross section and longitudinal steel distribution of the specimen.

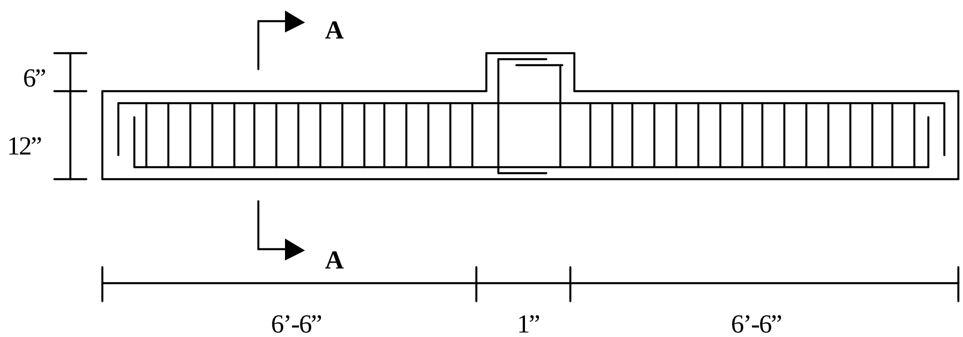

(a) Longitudinal Steel Distribution

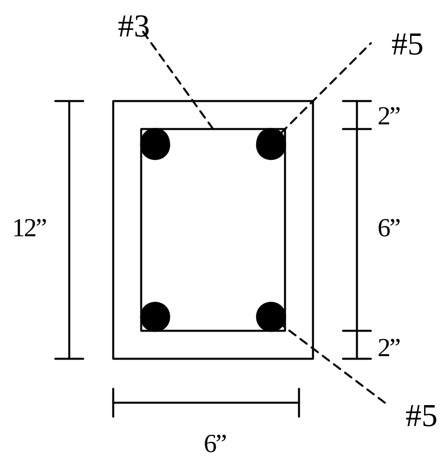

(b) Cross section (A-A)

Figure 3.1. Steel Distribution and Cross Section of RC Beams

All the specimens were constructed at a precast plant using conventional fabrication, curing, and transportation techniques. Dry sand blasting was performed by the contractor using industrial grade equipment in order to remove the fine particles and paste and leaving the coarse aggregate exposed. After testing cylinders of 3 in. radius by 6 in. Height obtained by coring a tested beam, the average compressive strength was 7500 psi. The longitudinal reinforcement consisted of four Grade 60 #5 steel reinforcing bars. The stirrups were made up from Grade 60 #3 steel bars spaced 5 in. center-to-center for Series A and B, and 10 in. for Series C. Three coupons of steel bars were tested under uniaxial tension in accordance with ASTM A370-90A. For the #5 reinforcing bars, the average yield stress was 62 ksi, the average ultimate was 102 ksi, and the average Modulus of Young was 28300 ksi. In the case of the #3 reinforcing bars, the values are 61 ksi for the average yield stress, 98 ksi for the average ultimate stress and 30100 ksi for the average Modulus of Young.

The RC block, in the midspan was intended to represent the intersection of a beam with a column, and even more, the intersection of a slab with a beam. However, it is important to mention that it is not possible to observe cover delamination in the latter case. The main reasons for using this configuration are to investigate how effective the strengthening is using CFRP sheets in the negative moment region, and in the future, combining flexural and shear by testing continuous beams.

Three different series of beams were tested (see Table 3.1). The cutoff points were located at the beginning of the pin and roller supports as shown in Figure 3.2. In series A, the beam span was 7 ft (2.13 m). Beam A0 was used as the control beam. The width of externally bonded reinforcement to the bottom of the beam was 6 in. (150 mm) for beams A1 to A5. The purpose of the different number of plies was to observe its incidence in the cover delamination failure. The width of the CFRP laminate in beams A6, A7 and A8 was 3 in. (75 mm). Beam A7 was strengthened with two plies of CFRP; whereas, beam A8 had six plies. The purpose of these configurations was to observe and compare their behavior to beams A1 and A3, strengthened with the same amount of CFRP but with different bonded areas.

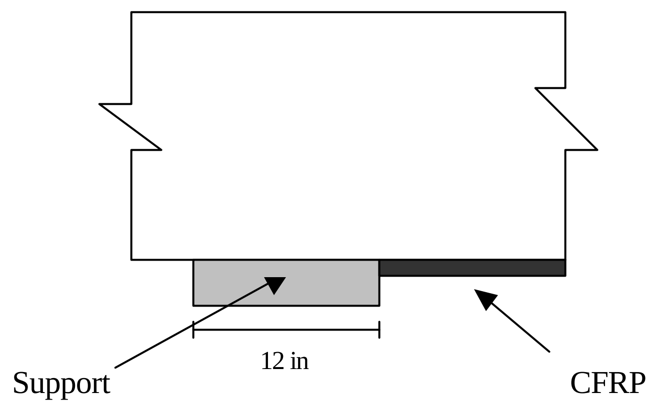

Figure 3.2. Location of Cutoff Points

Beams A4 and A5 were partially and totally wrapped (U-jacketing) at 90^0, respectively. The length to be wrapped in beam A4 was determined after the test results of beam A3, which showed a horizontal crack running approximately 2 ft (0.60 m) from the cut-off point of the sheets. The purpose of testing a partially wrapped beam was to improve the capacity of beam A4 by delaying the cover delamination failure. In the beam A5, the purpose was to compare partial to total wrapping.

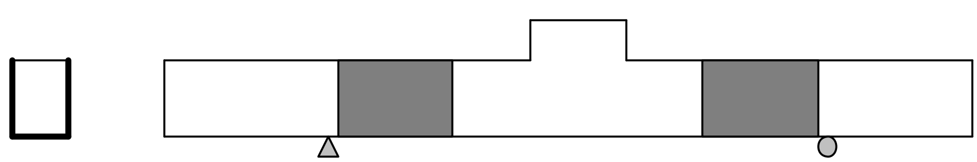

(a) Beam partially wrapped

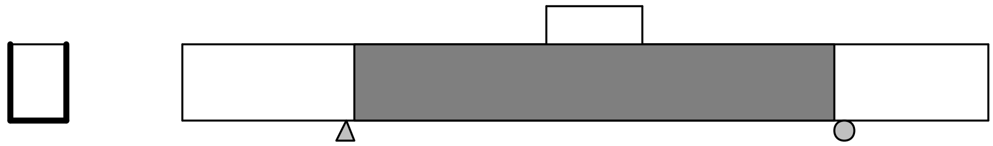

(b) Beam totally wrapped

Figure 3.3. Beams with U-Jacketing

Series B consisted of four beams, their testing span was 13 ft (3.96 m). Beam B1 was strengthened with one ply of CFRP of 6 in. (150 mm) in width. In beams B2 and B3, the width was 3 in. (75 mm) with one and two plies, respectively. The objective in this series was to compare the behavior of beams similarly strengthened but with different bonded areas.

Three beams were tested in series C. The test span was 7 ft (2.13 m), similarly to series A. The only difference compared to that series is the stirrup spacing, which was 10 in. (250 mm). The purpose of this series was to observe the influence of stirrup spacing on the failure mode.

Table 3.1. Experimental Program

		width=6 in			width=3 in				
NUMBER OF PLIES	0	1	2	3	1	2	6		
Span = 7 ft	A0	A1	A2	A3	A6	A7	A8	No Wrapping	Series A
				A4				Partially Wrapped	
				A5				Totally Wrapped	
Span = 13 ft	B0	B1			B2	B3		No Wrapping	Series B
Span = 7 ft	C0	C1		C2				No Wrapping	Series C

3.2. CARBON FIBER REINFORCED POLYMER (CFRP) SHEETS

Carbon fiber sheets Replark 30, provided by Mitsubishi Chemical Corporation were employed in this research. Replark 30 is a prepreg carbon fiber sheet where the fibers are unidirectionally oriented. The sheet has a paper backing, which serves to keep the fibers in place. According to the manufacturer's information the tensile strength is 493 ksi, the modulus of elasticity is 33400 ksi, and the design thickness is 0.0065 in. In tension, the CFRP sheets have a linear elastic behavior up to failure. No independent tests were performed in order to corroborate these values. According to tests performed at the University of Bologna, Italy (Nanni, Di Tomasso, Arduini, 1997)), the mechanical properties of the epoxy resin or adhesive were 290 ksi for the modulus of elasticity and 0.36 for the Poisson's ratio.

3.2.1. Installation Process. The strengthening work consists of CFRP sheets attached to the surface of concrete by manual lay-up. The procedure employed to apply the CFRP sheets was that recommended by the manufacturer (Mitsubishi Chemical Corporation, 1994), which can be summarized as:

- A surface primer was applied to the concrete and allowed to dry for 4 hours. The main purpose of using a primer is to fill micro-cavities on the surface of the concrete.
- The putty is applied in order to level the uneven surface present on the concrete. The putty was allowed to cure for 4 hours.
- A first layer of impregnating resin was applied. The CFRP sheets were adhered to the concrete using this epoxy resin, which was mixed and applied to the concrete in a thin uniform layer using a roller.

- The carbon fibers were cut to the required length and width using scissors. Once, the sheet was in place, it was press down using a “bubble roller”, which eliminates the entrapped air between the fibers and epoxy resin.
- After the paper backing was removed, a second layer of impregnating resin was applied. The last two steps, application of epoxy resin and sheets, were repeated in the case of multiple plies. The CFRP sheets were allowed to cure for 24 hours at room temperature before putting into storage.

A scheme of the laminate is shown in Figure 3.4.

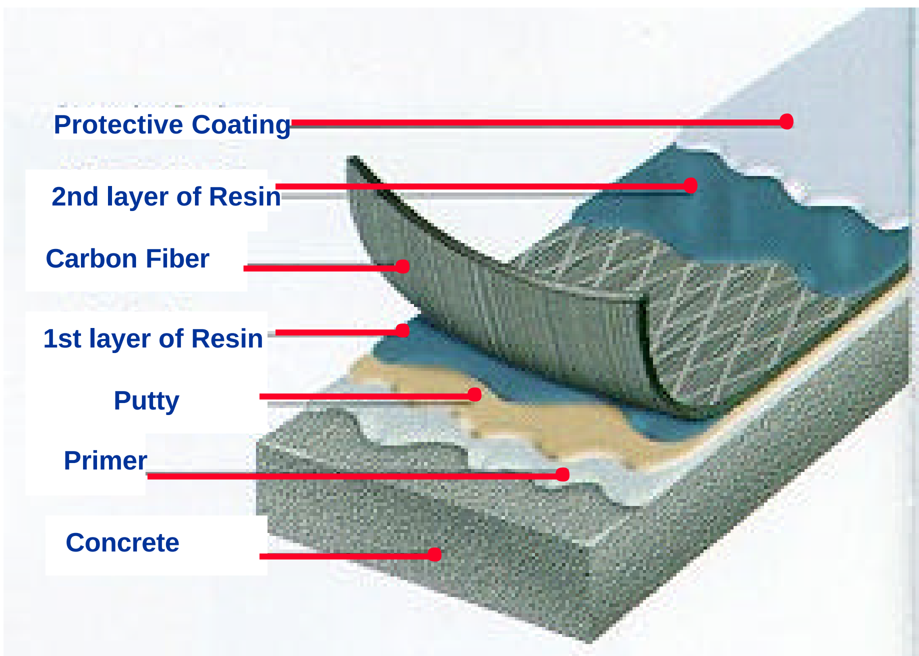

Figure 3.4. Installation of CFRP Sheets

3.2.2. Total Thickness of the Sheet System. The thickness of the sheet system plays an important role in the mode of failure to be observed, which will be discussed in one of the analytical approaches studied in Chapter 5. Therefore, it is important to estimate the thickness of primer, putty, and epoxy layers as well as the thickness of FRP sheets.

In order to estimate these values, samples obtained from beams already tested were analyzed at the Materials Research Laboratory at the University of Missouri - Rolla using a Scanning Electron Microscope (SEM). The SEM is a microscope that uses electrons rather than light to form an image. By employing a SEM, more control in the amount of magnification can be obtained. Figure 3.5 summarizes the result of the analyses.

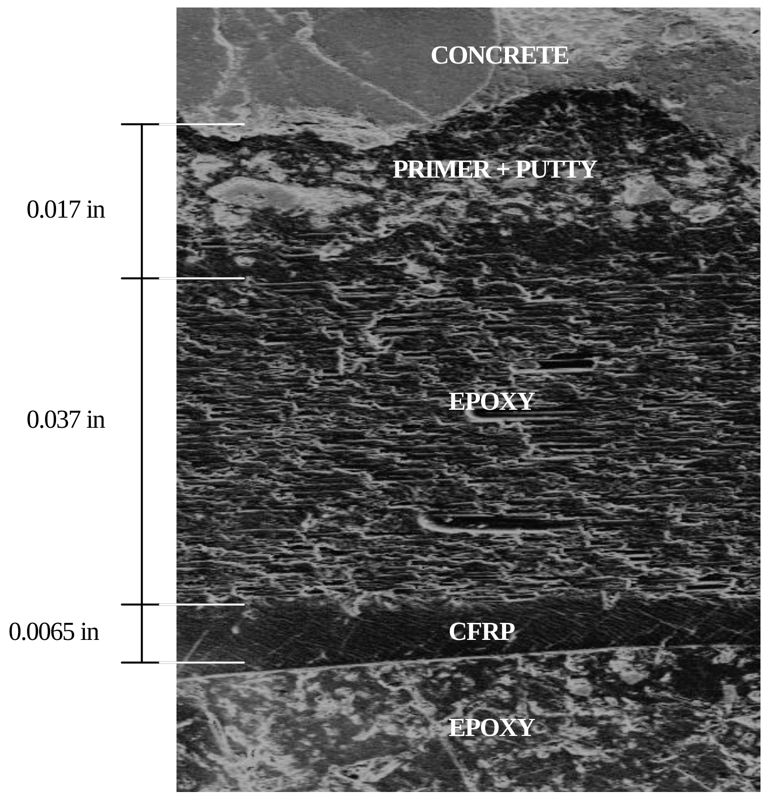

Figure 3.5. Thickness of Sheets

3.3. TEST SETUP

All beams were tested as simply supported beams under one symmetrical load with a total span of 7 ft for Series A and B, and 13 ft for Series C, as shown in Figure 3.6.

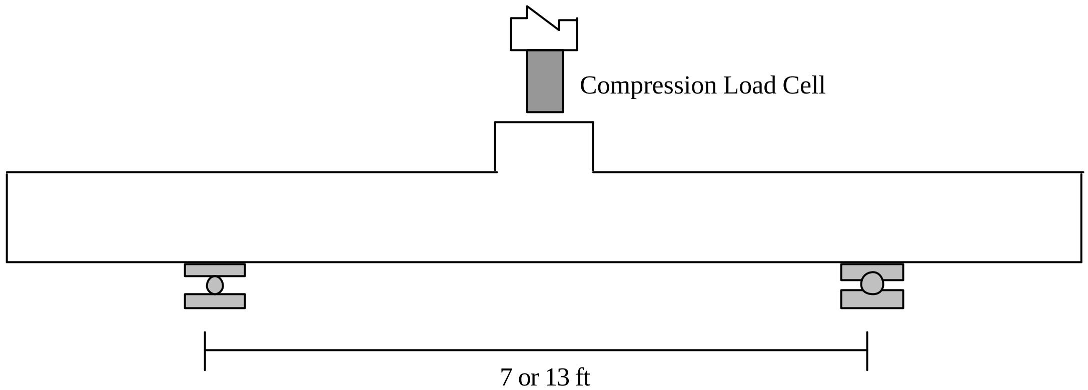

Figure 3.6. Test Setup

The tests were conducted at the Structural Engineering Research Laboratory at the University of Missouri-Rolla. The test setup consisted of two groups of equipment: the loading machine and the test bed. They can be observed in Figure 3.7, labeled as 1 and 2, respectively.

Figure 3.7. Loading Machine and Test Bed

A loading Machine of 400 kips capacity, Baldwin Universal Testing was used in order to apply the concentrated load. As shown in Figure 3.8, the loading machine consisted of a screw driven reaction cross-head at mid-height and the control panel, labeled as 1 and 2, respectively.

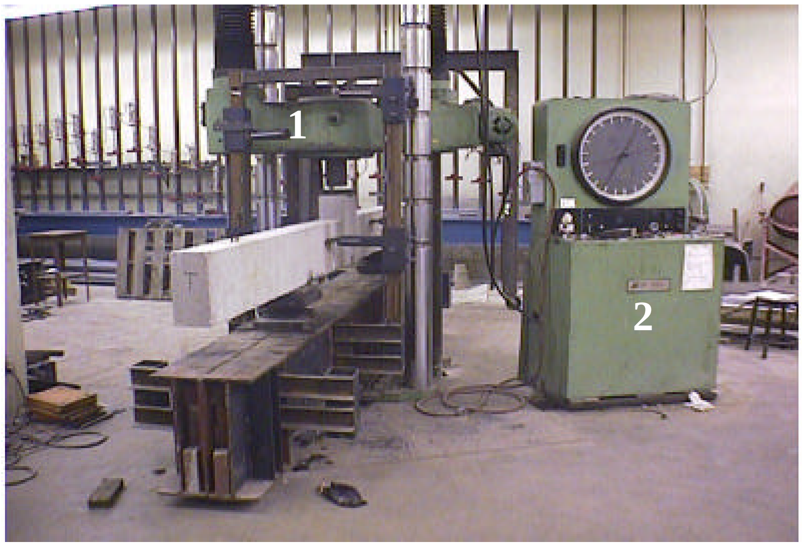

Figure 3.8. Screw Driven Reaction and Control Panel

The test bed consisted of three elements: the test bed itself, the lateral supporting system and the roller supports for the beam. The test bed was a built-up section of two W21x62 wide flange sections and an intermediate ½ in. by 21in. web plate, total length being 14 feet. The lateral supporting system provided lateral support to the RC beams during and after the tests. The lateral supports consisted of four steel columns with adjustable collars. The specimens were supported by heavy-duty pin roller supports on a span of seven feet. These supports provided bearing, frictionless rotational and translational action. The hinge action was provided by a 1 inch solid cold-formed steel rod. The hinges were greased before testing in order to provide a smooth action.

3.4. TEST PROCEDURE

3.4.1. Loading. The load was applied in cycles of loading and unloading. A cycle before cracking of concrete was done in order to verify both the mechanical and electronic equipment were working properly. Two cycles before yielding of the steel reinforcement were done. After reaching this point, the number of cycles depended on the maximum expected load. By applying the load by cycles, the stability of the system can be checked.

3.4.2. Data Acquisition. The data coming from the load cell and the Linear Variable Differential Transducers (LVDTs) were collected by a data acquisition system at a frequency of one point per second. This system included a Data General Conditioner Rack and LABTECH (Laboratory Technologies Corp.) data acquisition software. The system has the capability of reading up to 32 data channels. For the tests carried out as part of this research, seven channels were used; one for load, which was recorded using a 500 kips capacity load cell, and six for displacement readings, which were recorded through the LVDTs. As shown in Figure 3.9, one LVDT was placed at each support in order to take into account the support settlement (LVDTs 1 and 6). Two LVDTs were placed at fourths of the span (LVDTs 2 and 5) and two more at the midspan to read the deflection at those points (LVDTs 3 and 4).

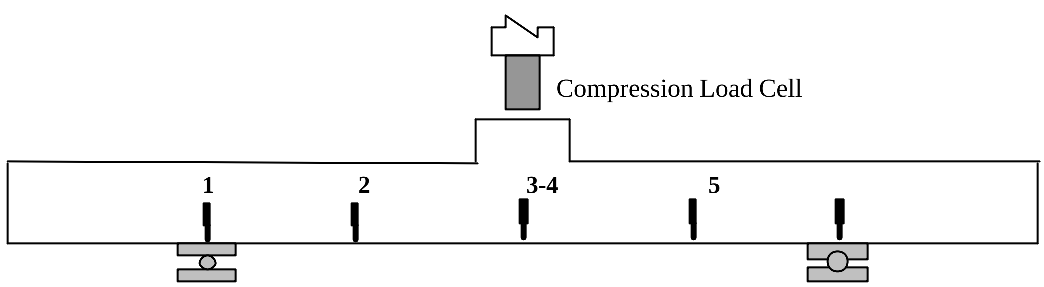

Figure 3.9. Location of LVDTs

4. TEST RESULTS

Two mechanisms within the concrete cover delamination failure were observed: one starting at the cutoff point of the CFRP sheets, hereafter referred as Failure Mode I; and a second one starting at an intermediate crack, hereafter called Failure Mode II.

4.1. SERIES A

Variables such as the number of plies of CFRP, bonded area, and contribution of U-jacketing (wrapping) were studied in this series. Nine beams were tested, the experimental results are described below.

Failure in the control beam A0 was typical that of under-reinforced RC flexural members, which is characterized by yielding of steel rebars followed by concrete crushing. Table 4.1 summarizes the predicted, experimental values for flexural capacities as well as the mode of failures obtained in each test. The failure in beam A1 was according to Mode II (see Figure 4.1).

Figure 4.1. Final Failure in Beam A1

Table 4.1. Flexural Capacities and Modes of the Failure – Series A

BEAM	PREDICTED FLEXURAL CAPACITY (ft-kips)	EXPERIMENTAL FLEXURAL CAPACITY (ft-kips)	MODE OF FAILURE
A0	42.0	41.6	Concrete Crushing
A1	57.2	57.2	Failure Mode II
A2	77.4	66.7	Failure Mode II
A3	95.4	67.6	Failure Mode I
A4	95.4	77.1	Failure Mode II
A5	95.4	83.1	Cover Delamination
A6	48.0	55.4	CFRP Rupture
A7	57.2	67.6	Failure Mode II
A8	95.4	77.1	Failure Mode I

In beam A2, the first cracks were vertical; they did not open up as wide as the control beam A0. The failure was caused by cover delamination, similar to beam A1. In beam A3, the failure was caused by cover delamination at the cut-off point of the sheet (Mode I), as shown in Figure 4.2.

Figure 4.2. Final Failure in Beam A3

The behavior of beams A3 and A4 is similar until the failure of the beam A3 (see Figure 4.3). It is after this point where the contribution of the U-jacketing is evident. The use of the U-jacketing delayed the cover delamination failure. Beam A5 failed by cover delamination. The test of this beam showed that the failure load was enhanced compared to A3 and A4 and the ultimate deflection was less than in the case A0.

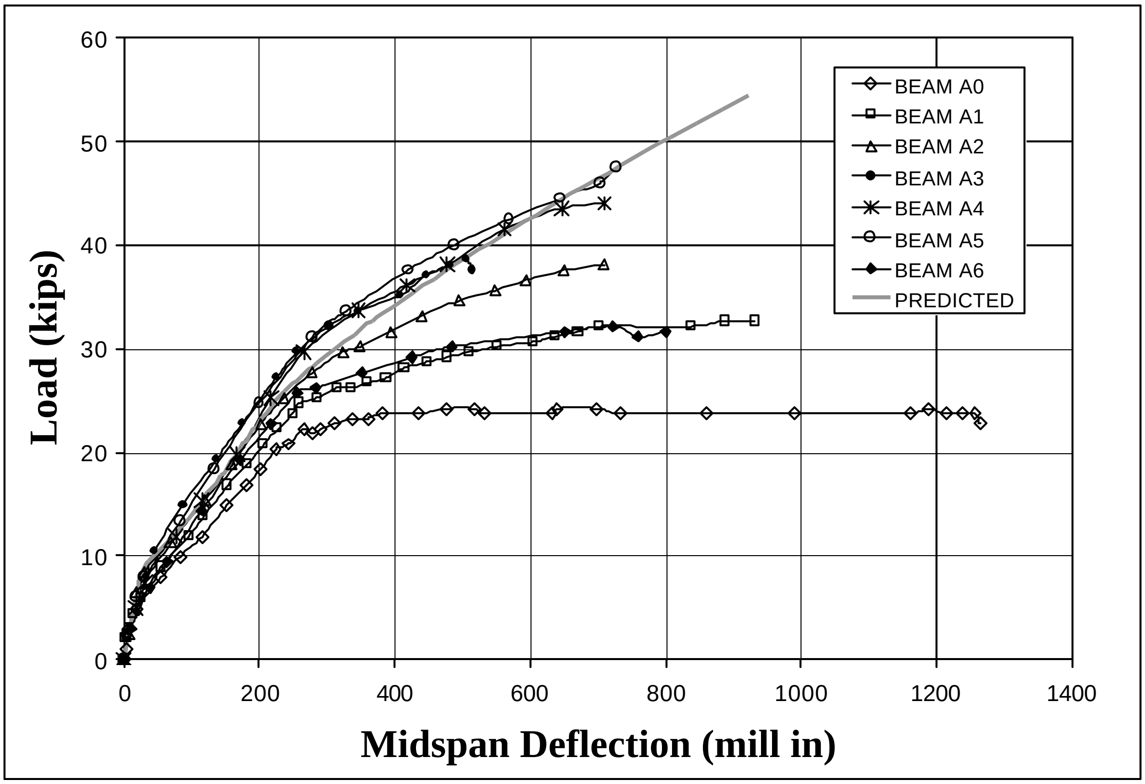

Figure 4.3. Load vs. Deflection Curves – Series A

Even though, beam A6 had half of the amount of external reinforcement as compared to beam A1, both exhibited similar capacities. Beam A6, which failed due to CFRP rupture (see Figure 4.4), exceeded the predicted capacity. From the results obtained in beams A7 and A8, it is concluded that beams strengthened with the same amount of CFRP on different bonded areas have similar behavior.

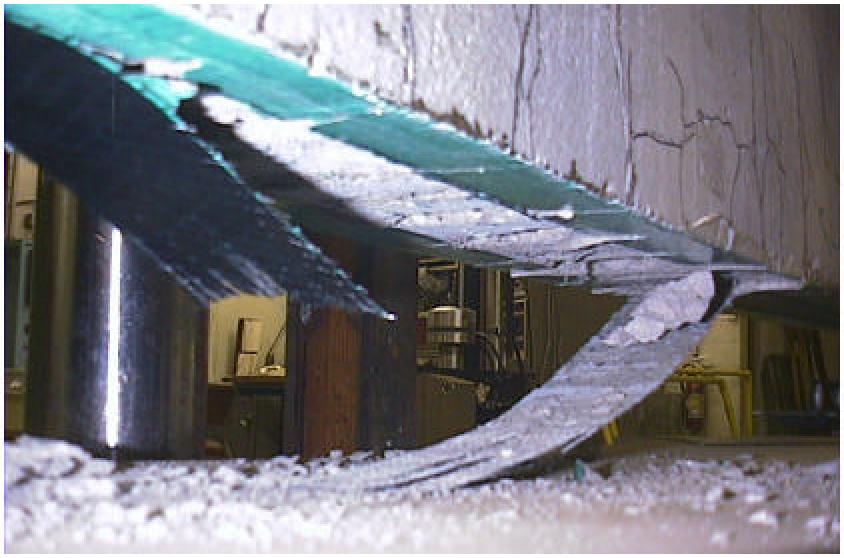

Figure 4.4. Final Failure in Beam A6

All the strengthened beams showed important increases in flexural stiffness and ultimate capacity as compared to the control beam A0. In order to quantify the flexural stiffness of the beams, average values of the slope of the load deflection curves after the concrete cracks and before the steel yields were taken.

The flexural stiffness for a simply supported beam with a concentrated load, applied at the midspan can be computed as $EI = \frac{L^3}{48} \times K$, where L is the length of the span and K is the slope of the Load vs. Deflection Curve. As shown in Table 4.2, the stiffness of Beam A1 increased 13%, the stiffness of Beam A2 increased, roughly, 15%; while the Beam A3 displayed a 28% increase. In the Beams A4 and A5, the stiffness is roughly the same as that found in Beam A3 because the contribution of the U-Jacketing is observed once Beam A3 reached the final failure as shown in Figure 4.3

.

Table 4.2. Flexural Stiffness of Beams – Series A

BEAM	**FLEXURAL STIFFNESS (kips-ft^2)**	**PERCENT INCREASE**
A0	6174	---
A1	6946	13%
A2	7117	15%
A3	7889	28%
A6	7024	14%

As expected, after steel yielding, the flexural stiffness increased when the number of plies of CFRP was increased.

Considering ductility (μ) is defined as the deflection at the ultimate state of failure (δu) divided by the deflection at the yielding of steel (δy). It can be observed from Table 4.3 that the control beam A0 had a ductility of 4.3. On the other hand, the ductility in the strengthened beams decreased, gradually, when the number of plies was increased (see Table 4.3 and Figure 4.3). However, owing to the employment of the U-jacketing the ductility increased in Beams A4 and A5 because the cover delamination failure was delayed.

From the point of view of design and following the philosophy of ACI 318-95, sections with significant loss of ductility must be compensated with a higher strength reserve, which is accomplished by applying a strength reduction factor of 0.70 to brittle sections instead of 0.90 for ductile sections.

Table 4.3. Ductility of Beams

BEAM	d**y (mill in)**	d**u (mill in)**	m
A0	293	1264	4.3
A1	272	932	3.4
A2	314	661	2.1
A3	270	509	1.9
A4	302	653	2.2
A5	279	726	2.6
A6	254	801	3.2

Regarding to the ultimate capacity, the Beams A4 and A5 displayed increases over the Beam A3 of 15% and 23%, respectively. In addition, loads associated to cracking and yielding are, also, increased with the number of plies.

During the tests, it was observed that the employment of CFRP sheets delayed the presence of the first visible cracks, and also, the distance between flexural cracks decreased when the number of plies of CFRP increased. In addition, there is evidence from previous works that the crack widths are reduced (Chaallal, Nollet, Saleh, 1998). Finally, the cover delamination failure, observed in beam A3, started at the end of the bonded sheets, which was caused by the high stress concentration in that zone.

4.2. SERIES B

The objective of this series was to compare the behavior of strengthened beams with different testing spans, 13 ft versus 7 ft. Four beams were tested, the experimental results are shown in Figure 4.5. The predicted and experimental values for flexural capacities as well as the mode of failures are shown in Table 4.4.

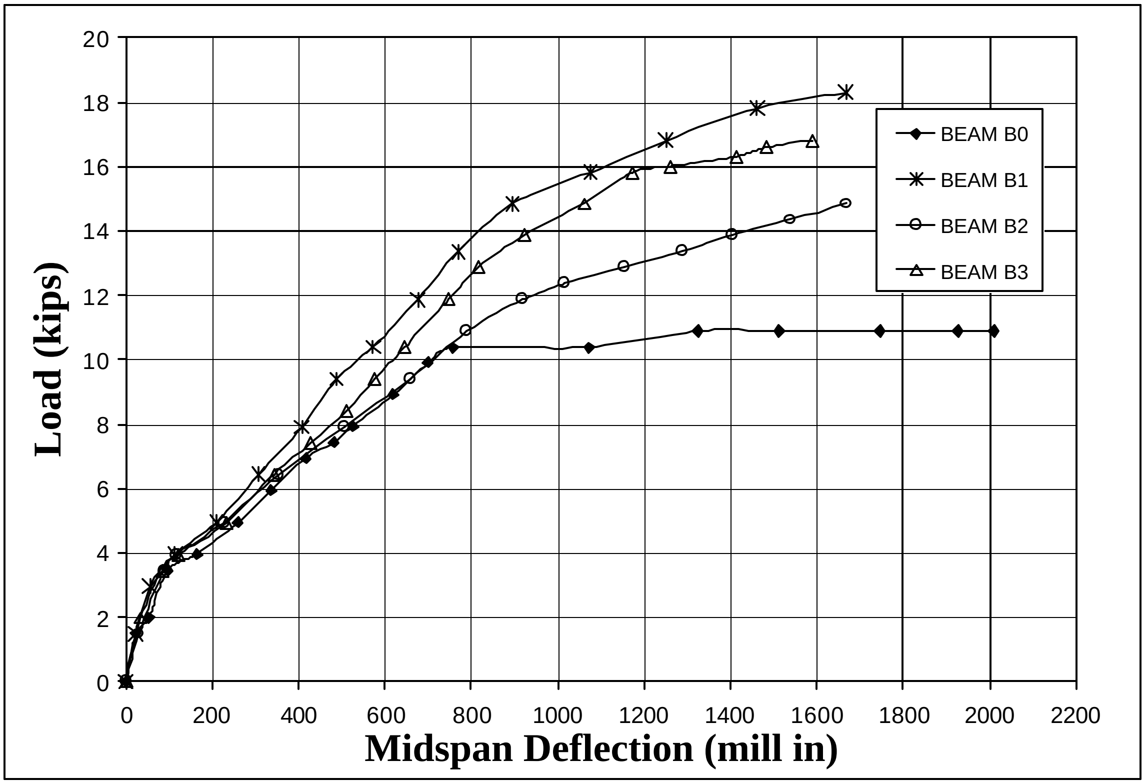

Figure 4.5. Load vs. Deflection Curves – Series B

Table 4.4. Flexural Capacities and Modes of the Failure – Series B

BEAM	PREDICTED FLEXURAL CAPACITY (ft-kips)	EXPERIMENTAL FLEXURAL CAPACITY (ft-kips)	MODE OF FAILURE
B0	42.0	35.4	Concrete Crushing
B1	57.2	59.5	Concrete Crushing
B2	50.8	48.2	CFRP Rupture
B3	57.2	54.7	Concrete Crushing

By plotting a normalized load vs. deflection curve, the behavior of beams A7 and B3 can be compared (see Figure 4.6). It can be observed that up to yielding of the steel reinforcement, the specimens behaved in similar manner.

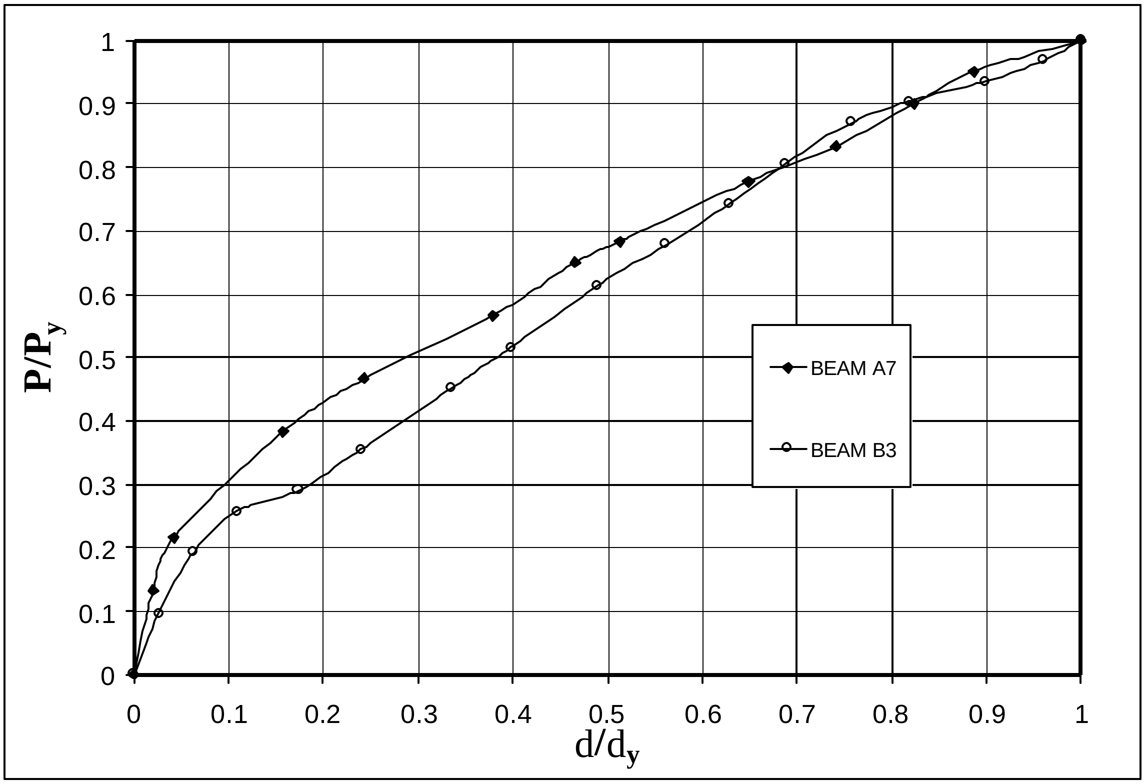

Figure 4.6. Normalized Load vs. Deflection Curve (Up to yielding)

4.3. SERIES C

The purpose of this series was to observe the influence of the stirrup spacing on the concrete cover delamination failure. Based on the results of corresponding beams in series A and C, it was concluded that there was no significant influence in the mode of failure. The experimental results are shown in Table 4.5 and Figure 4.7.

Table 4.5. Flexural Capacities and Modes of the Failure – Series C

BEAM	PREDICTED FLEXURAL CAPACITY (ft-kips)	EXPERIMENTAL FLEXURAL CAPACITY (ft-kips)	MODE OF FAILURE
C0	42.0	48.5	Concrete Crushing
C1	57.2	60.6	Failure Mode II
C2	95.4	62.3	Failure Mode I

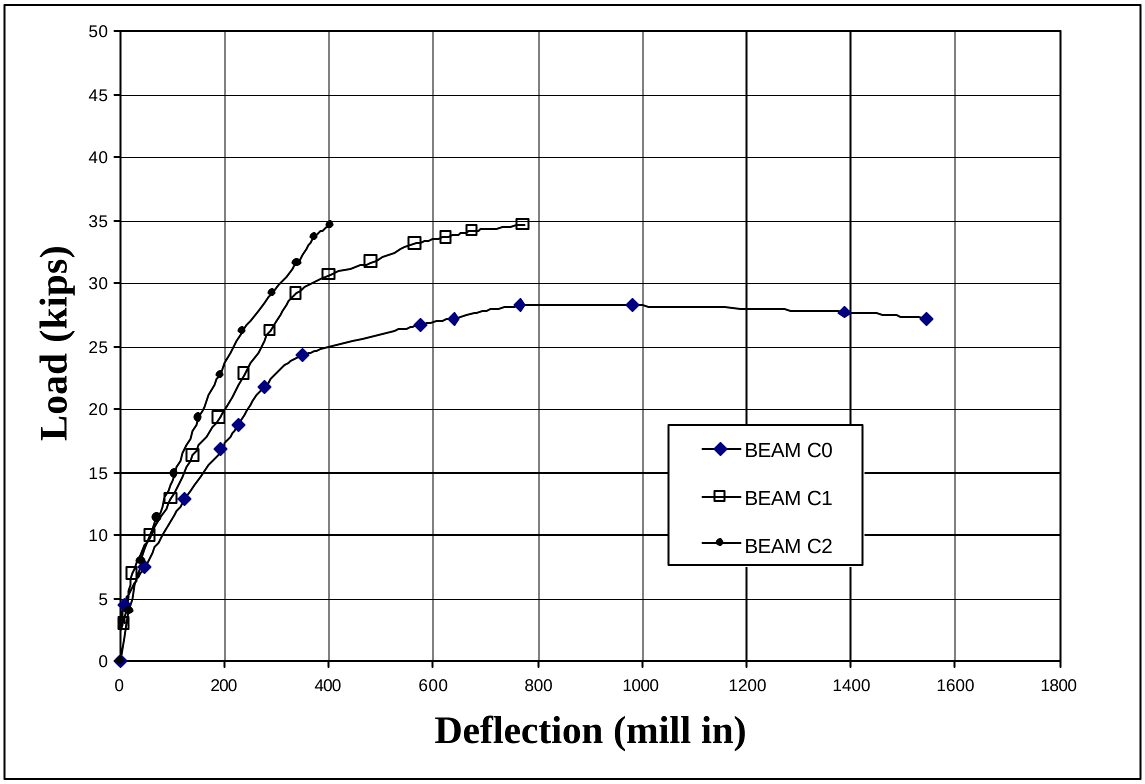

Figure 4.7. Load vs. Deflection Curves – Series C

5. ANALYTICAL STUDY

It has been observed from experimental evidence that in many cases beams strengthened in flexure with FRP sheets fail prematurely (Takahashi, Sato, Ueda, 1997; Chaallal, Nollet, Saleh, 1998). This failure is caused by the concrete cover delamination of the FRP sheets. One of the main concerns of this thesis is to give an analytical explanation for this kind of failure, and intend to predict it.

As it was mentioned in Section 1, two modes of failure were observed within the concrete cover delamination failure. For simplicity, they are to be called Failure Mode I and Failure Mode II. Failure Mode I refers to failure caused by cover delamination starting at the cutoff of the sheets; whereas, Failure Mode II refers to failure caused by concrete cover delamination starting at an intermediate crack and developing towards the beam midspan.

5.1. MECHANISM OF FAILURE MODE I

The curtailment of the laminate adjacent to a support originates a high concentration of normal and shear stresses at the cutoff point of the sheet. Previous research (Deshmukh, 1996) for RC beams strengthened with either steel or FRP plates has shown that the magnitude of these stresses depends on the geometry of the reinforcement, the engineering properties of the adhesive, and tensile and shear strength of the concrete. In the case of RC beams strengthened with FRP sheets, the geometry refers to the number of plies (thickness of the FRP sheets) as well as the distance from the support to the edge of the sheets. Consider an element, which is isolated from the beam as shown in Figure 5.1.

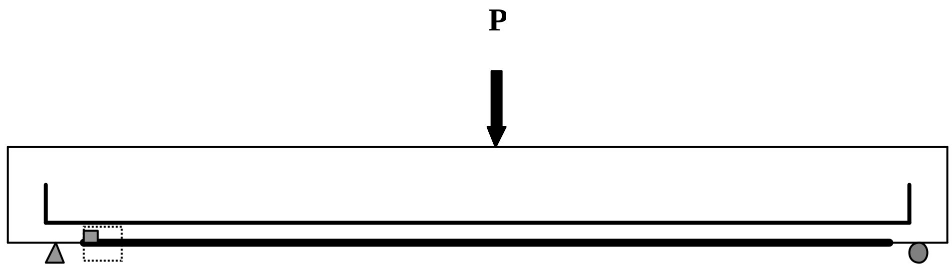

Figure 5.1. Beam From Which the Element is Isolated (Failure Mode I)

The stress distributions for normal and shear stresses needed to ensure the equilibrium of the mentioned element at the level of the steel reinforcement, as well as the existing forces, are shown in Figure 5.2.

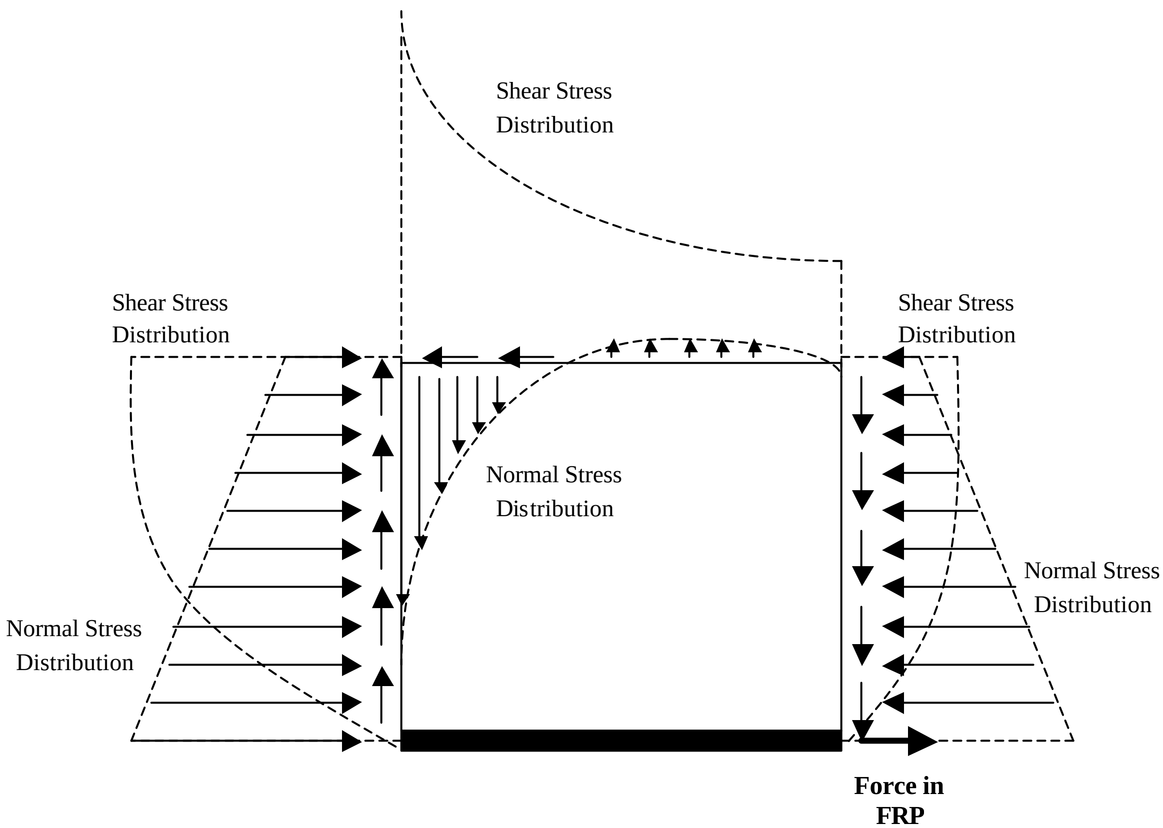

Figure 5.2. Free Body Diagram of the Isolated Element

The stress distributions on the horizontal plane are those obtained from the analytical models described in Section 2. As mentioned, they were derived by assuming fully composite action between concrete and the external reinforcement and uncracked section. The failure caused by Failure Mode I starts at the ends of the sheets (see Figure 5.3) and is induced by the high concentrations of stresses at that point. The development of the horizontal crack depends on flexural cracks, shear cracks and bond stresses along the steel reinforcement (Arduini, Di Tomasso, Manfroni, 1995). Previous studies relative to bonded plates (Oehlers, Moran, 1990) have shown two kinds of failures. One failure was caused by the peeling-off of the plate, leaving the concrete cover intact, and another failure was caused by concrete cover delamination, which leaves the steel reinforcement exposed. RC beams strengthened with FRP sheets which fail by peeling-off beginning from the cutoff point have not been reported; whereas concrete cover delamination, as shown in Figure 5.3, is common.

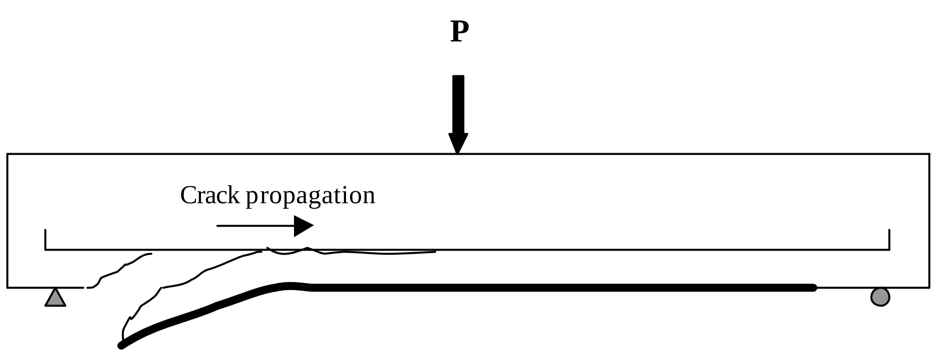

Figure 5.3. Crack Development for Failure Mode I

5.1.1. Analytical Approach. The normal and shear stresses acting on a volume element at the cutoff point of the FRP sheets are shown in Figure 5.4.

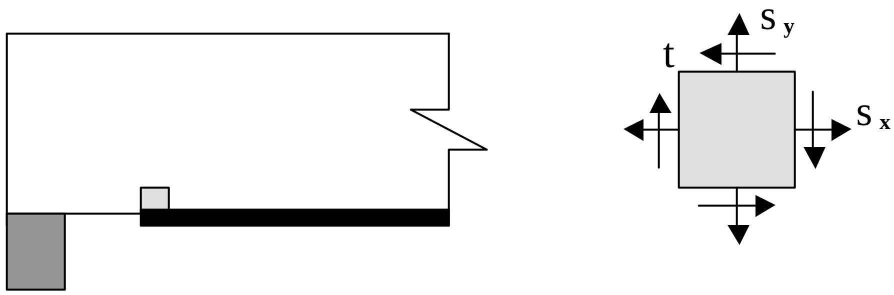

Figure 5.4. Stresses Acting at Cutoff Point of FRP Sheets

The expressions derived by Roberts (1989) at the FRP curtailment for the shear and normal stresses, equations (15) and (16) in Section 2, can be rearranged and simplified. Considering the employment of sheets instead of plates, and that the width of the FRP sheet (*wf*) must be equal to the width of the adhesive (*ba*), the following equations can be derived from equation (3) and (9) in Section 2.

$$t = \left[V + (Ga \frac{ba}{ta} \cdot \frac{1}{Ef\, wf\, tf})^{1/2} M \right] \frac{wf\, tf}{I\, ba} \tag{44}$$

$$s = ttf \left(\frac{Eaba}{ta} \cdot \frac{1}{4Ef(\frac{wf\, tf^3}{12})} \right)^{1/4} \tag{45}$$

Simplifying, the following expressions for the stresses at the cutoff point of the sheets can be derived:

Shear Stress

$$\tau = \left(V + M\left(\frac{Ga}{Ef\, tf\, ta}\right)^{1/2}\right)\frac{tf}{I}\bar{h}\left(\frac{Ef}{Ec}\right) \qquad (46)$$

Normal Stress in ‘y’ direction

$$\sigma_y = \tau\left(\frac{3Ea\,tf}{Ef\,ta}\right)^{1/4} \qquad (47)$$

In addition;

Normal Stress in ‘x’ direction

$$\sigma_x = \frac{M\bar{h}}{I} \qquad (48)$$

where:

V = shear force at the end of the FRP sheets

M = moment at the end of the FRP sheets

I = moment of Inertia of the uncracked section transformed to concrete

$\bar{h}$ = neutral axis for uncracked section (measured from the bottom)

Ef = modulus of elasticity of FRP sheets

Ec = modulus of elasticity of concrete

Ga = shear modulus of adhesive

tf = thickness of FRP sheets

ta = thickness of adhesive

The failure is assumed to begin when the maximum principal stress σ_p equals the modulus of rupture of concrete, which will be taken as $8.3\sqrt{f'c}$ (Mirza, Hatzinikolas and MacGregor, 1979).

$$s_p = \frac{s_x + s_y}{2} + \sqrt{\frac{(s_x - s_y)^2}{4} + t^2} \tag{49}$$

The angle θ_p, defined in equation (67), expresses the orientation of the principal plane where the initial crack travels through.

$$q_p = \arccos\left(\frac{s_x - s_y}{\sqrt{\left(\frac{s_x - s_y}{2}\right)^2 + t^2}} \right) \tag{50}$$

This angle indicates the initial crack orientation, which becomes horizontal at the level of the steel reinforcement where the weakest horizontal surface, produced by the reduction in the concrete area due to the presence of the steel bars is located (see Figure 5.5). The analytical values of θ_p are shown in Appendix D; for beams inclined to fail in Failure Mode I these values are around 15^o. The flatness of this angle may facilitate the appearance of the horizontal crack.

5.1.2. Validation of the Analytical Approach. The process to pursue in order to validate the analytical approach can be summarized as follows:

1. The thickness of the adhesive and sheets are estimated. These values are based on those obtained by a SEM, as it was described in Section 3.

2. By substituting these values along with those corresponding to the internal forces at the cutoff point and the geometric and material properties in equations (46), (47) and (48), the shear and normal stresses at the curtailment of the sheets can be calculated.
3. A maximum principal stress associated to the existing state of stress is quantified. Whenever the value of this principal stress exceeds the modulus of rupture of concrete, estimated as $8.3\sqrt{f'c}$, Failure Mode I occurs.

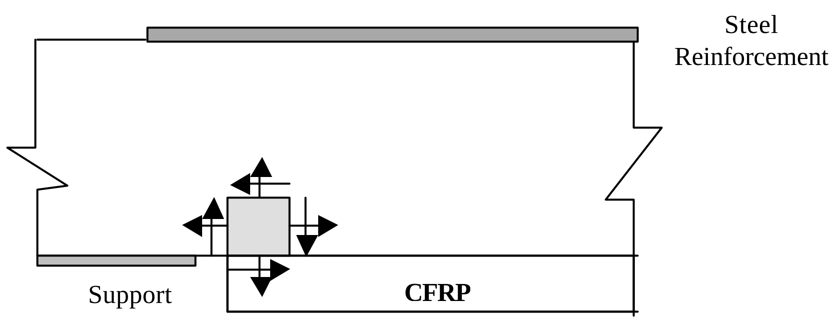

(a) Normal and shear stresses acting on element at cutoff point

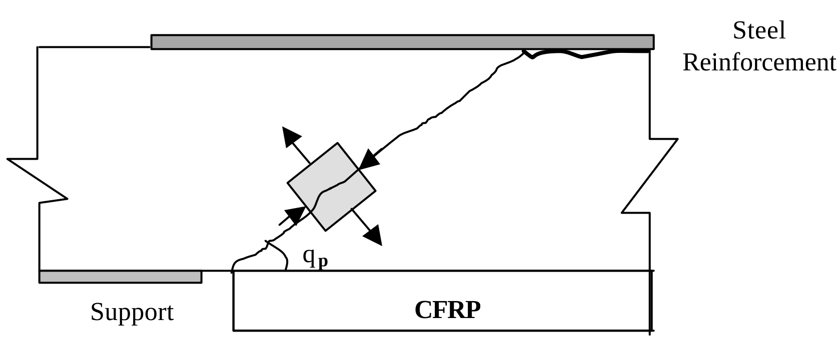

(b) Principal stresses acting on element at cutoff point

Figure 5.5. Cracking Development at the Cutoff Point

By using the test configuration employed in this investigation and estimating a load of 37.5 kips, the shear force and bending moment at this level are:

$$V = \frac{P}{2} = \frac{37.5\,kips}{2} = 18.75kips$$

$$M = V.Lo = (18.75\ kips)(6\ in) = 112.5\ kips\text{-}in$$

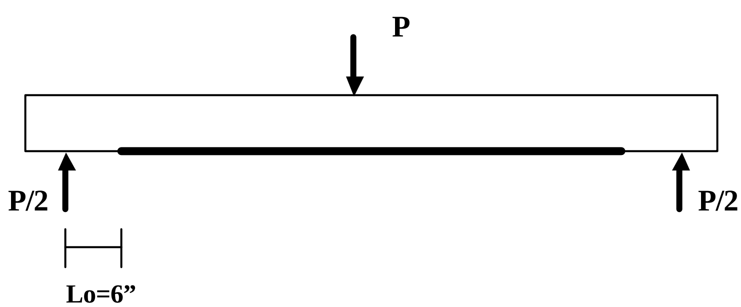

Figure 5.6. Test Configuration

where, Lo represents the distance between the center support and the cutoff point.

The cross section of an RC beam strengthened with 3 plies of CFRP, which will be analyzed, is shown in Figure 5.7.

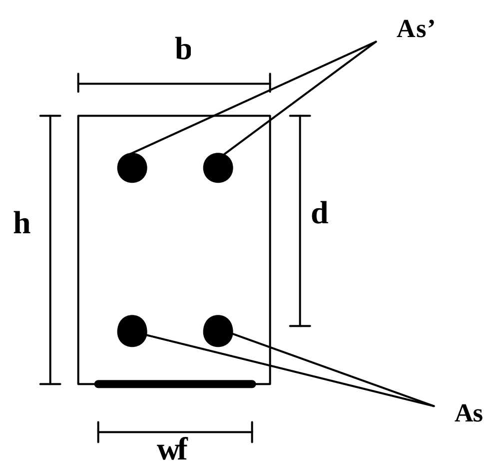

Figure 5.7. Geometry of the Cross Section Used for Validation

The geometric properties of the section are:

b = 6 in

h = 12 in

d = 10 in

As = 0.62 in^2

As' = 0.62 in^2

wf = 6 in

thickness of carbon fiber = 0.0065 in

The results of experimental and manufacturing data are:

Carbon Fiber

Ef = 33400 ksi

Epoxy

Ea = 290 ksi

? = 0.36

Ga = 107 ksi

Steel

fy = 62 ksi

Es = 28300 ksi

Concrete

f 'c = 7500 psi

Ec = $57\sqrt{f'c} = 4936$ ksi

- **Estimate thickness of the adhesive (ta) and sheets (tf)**

The thickness of the adhesive (ta) is equal to the summation of the thickness of primer, putty and first layer of epoxy resin.

ta = 0.020 + 0.040 = 0.060 in

If the contribution of the epoxy is not taken into accout, tf can be calculated as:

tf =3 (0.0065) = 0.020 in

- **Find centroid and moment of inertia in the uncracked section**

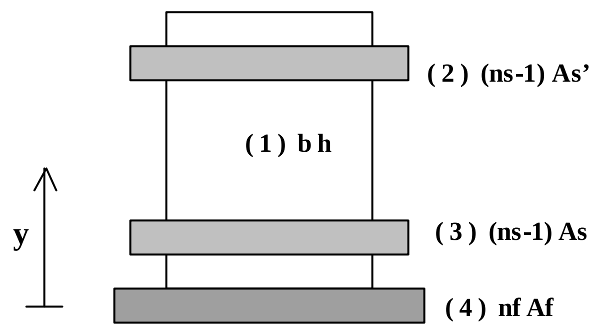

Figure 5.8. Uncracked Transformed Section

where:

(1): area of concrete

(2): transformed area of steel in compression

(3): transformed area of steel in tension

(4): transformed area of FRP

$$ns = \frac{Es}{Ec} = \frac{28300\,ksi}{4936\,ksi} = 5.73$$

$$nf = \frac{Ef}{Ec} = \frac{33400\,ksi}{4936\,ksi} = 6.77$$

The following table is obtained from Figure 5.8:

Table 5.1. Calculation of Geometric Properties

	A (in^2)	**$\bar{y}$ (in)**	**A . $\bar{y}$**	**($\bar{y}$ - $\bar{h}$)^2**	**I (in^4)**	**A . ($\bar{y}$ - $\bar{h}$)^2**	**I+A . ($\bar{y}$ - $\bar{h}$)^2**
1	72	6.01	432.70	0.17	864	0.26	864.26
2	2.934	10.01	29.37	16.49	---	48.38	48.38
3	2.934	2.01	5.90	15.52	---	45.54	45.54
4	0.792	----	---	35.39	---	28.02	28.02

$$\bar{h} = \frac{432.70 + 29.37 + 5.90}{72 + 2.934 + 2.934 + 5.663} = 5.95\,in$$

$$I = 864.26 + 48.38 + 45.54 + 28.02 = 986.21\,in^4$$

- **Find Shear and Normal Stresses**

By using equations (46), (47) and (48):

Shear Stress:

$$\tau = \left[(18.75\,kips) + (112.5\,kips\text{-}in)\left(\frac{107\,ksi}{(33400\,ksi)(0.020\,in)(0.060\,in)}\right)^{1/2}\right]$$

$$\left(\frac{0.020\,in}{986.21\,in^4}\right)(5.95\,in)\left(\frac{33400\,ksi}{4936\,ksi}\right) = 0.163\,ksi$$

Normal Stresses:

$$\sigma_y = (0.366\,ksi)\left[\frac{3(290\,ksi)(0.020\,in)}{(33400\,ksi)(0.060\,in)}\right]^{1/4} = 0.049\,ksi$$

$$\sigma_x = \frac{M\,\bar{h}}{I} = \frac{(112.5\,kips - in)(5.95\,in)}{(986.21\,in^4)} = 0.679\,ksi$$

In equations (66) and (67):

$$\sigma_p = \frac{(0.676 + 0.049)}{2} + \sqrt{\frac{(0.676 - 0.049)^2}{4} + (0.163)^2} = 0.721 ksi = 8.3\sqrt{f'c}$$

$$\theta_p = \arccos\left(\frac{0.679 - 0.049}{\sqrt{\left(\frac{0.679 - 0.049}{2}\right)^2 + (0.163)^2}} \right) = 14^0$$

\ Predicted load at failure is 37.5 kips.

As evidence of the validity of this process, the load vs. deflection curve for Beam A3 tested to failure is shown in Figure 5.9. The experimental value for the load P at failure was 38.6 kips. In this way, the results for the load P at failure for the experimental and theoretical values are very close. However, it is clear more tests are needed in order to obtain a complete validation.

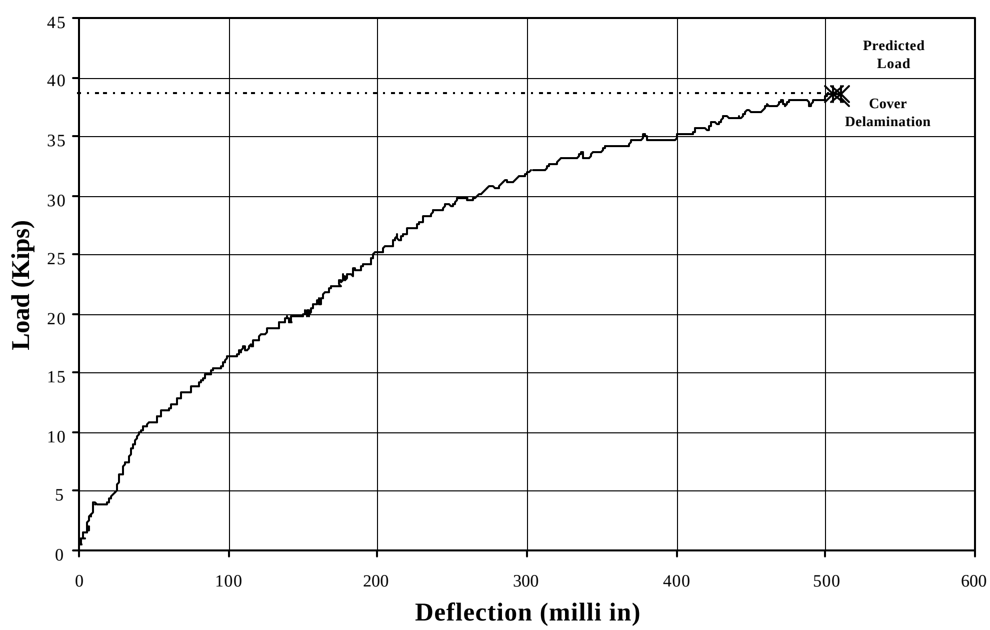

Figure 5.9. Experimental Validation for Ultimate Load

The analytical values for shear and normal stresses shown in Figure 5.10 facilitate the understanding of which mode of failure is probable. A detailed calculation for the different number of plies is shown in Appendix D. It can be observed from Figure 5.10 that the magnitude of the normal stress σ_y and shear stresses τ increases with the number of CFRP plies. This means that Failure Mode I may be observed when the laminate consists of more than one ply of CFRP. In the experimental phase of this investigation, Failure Mode I was observed only in the case of a RC beam strengthened with 3 plies of CFRP.

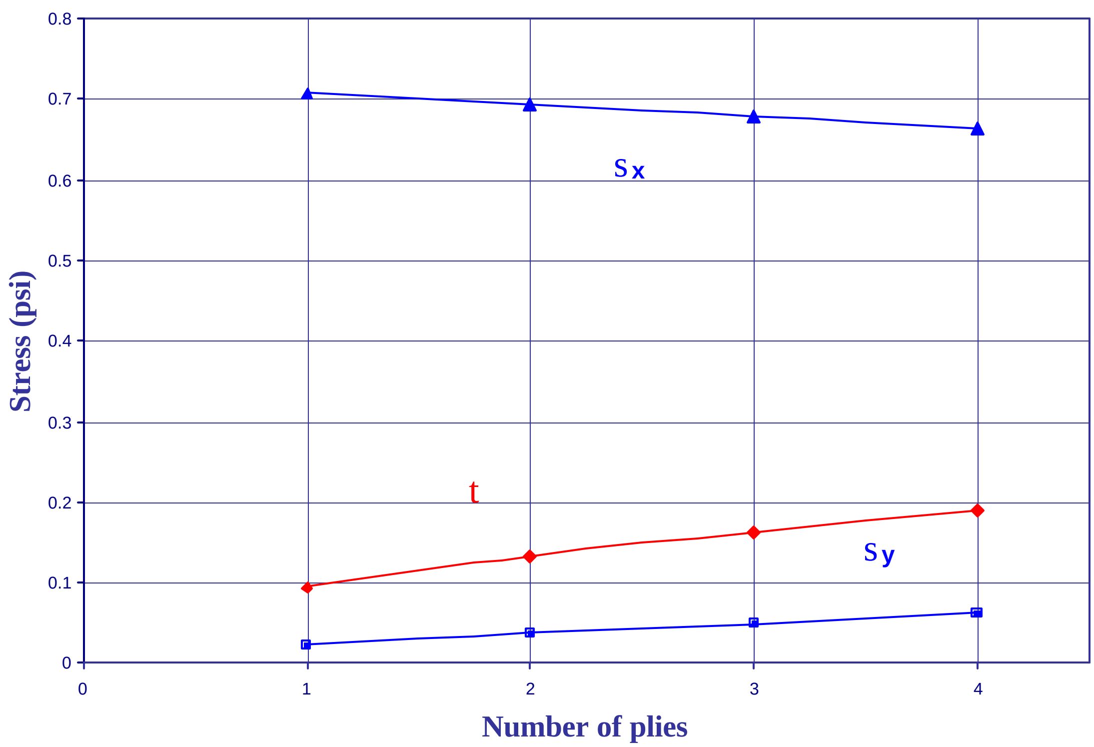

Figure 5.10. Influence of Number of Plies of CFRP on Shear and Normal Stresses

5.2. MECHANISM OF FAILURE MODE II

This failure is caused by cover delamination starting from one of the intermediate flexural cracks between the outermost crack and the maximum bending area. The horizontal crack is originated by splitting of concrete at the steel reinforcement level, and mainly, by normal and shear stresses at that level which are needed to ensure equilibrium. Figure 5.11 illustrates the cracking progression of this failure.

Stage 1 shows the flexural cracks for a certain level of external load. In stage 2, with further increases in external loads, the reduced area of bulk concrete at the level of the steel reinforcement pulls away from the rest of the beam after the horizontal crack appears starting at point F.

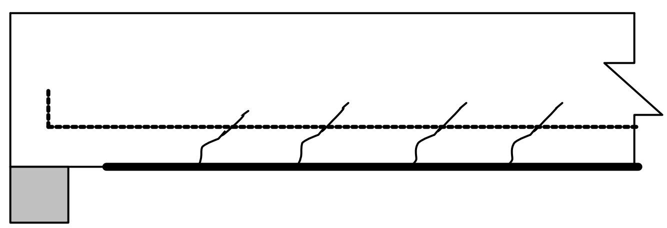

(a) Stage 1

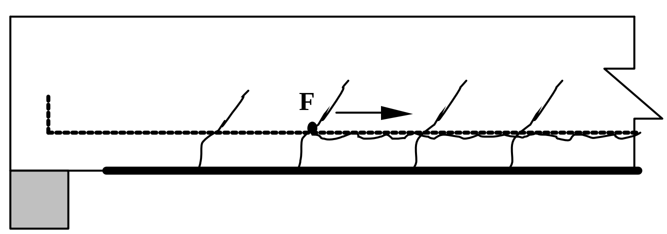

(b) Stage 2

Figure 5.11. Cracking Development for Mode II

As shown in Figure 5.12, an element between two flexural cracks is isolated. The distributions corresponding to shear, normal, and bond stresses, as well as the existing forces in the FRP sheets, are observed in Figure 5.13.

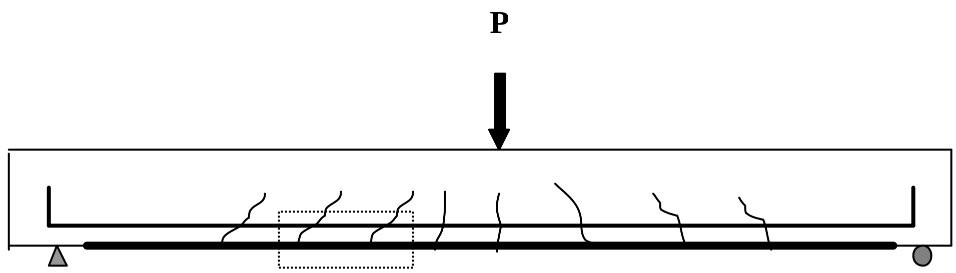

Figure 5.12. Beam From Which the Element is Isolated (Failure Mode II)

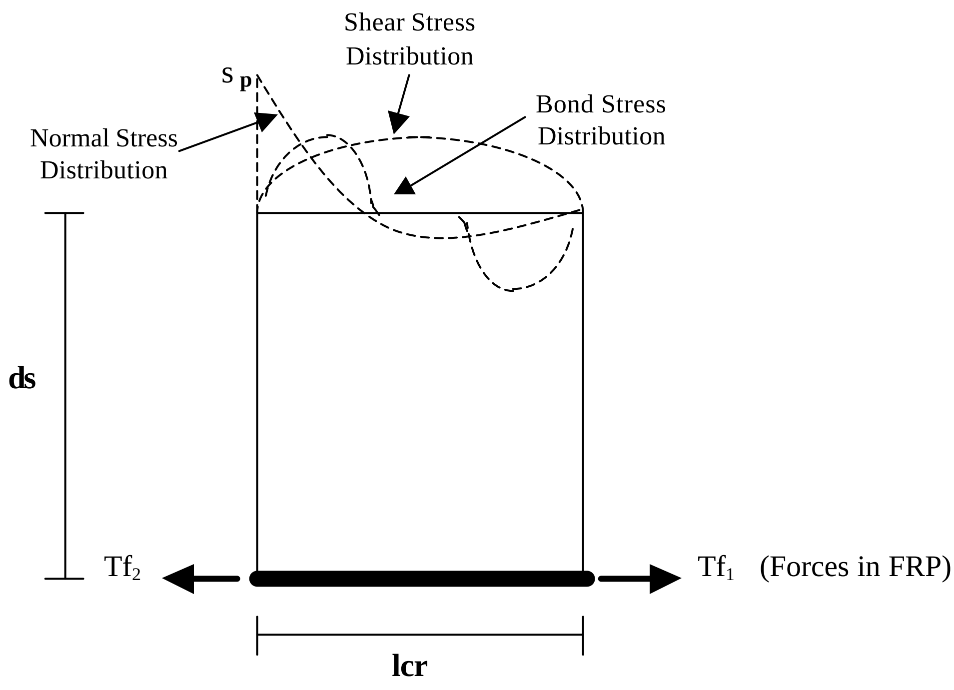

Figure 5.13. Free Body Diagram of the Isolated Element

Although more research is needed to obtain the exact distribution and magnitude of the normal and shear stresses that originate cover delamination, some assumptions can be made. For instance, the profile of the normal stress distribution may be similar to that found in the analytical models previously studied. Since there are no shear forces, due to the cracked section, acting on the vertical faces of the isolated element, the shear stresses at the edges of the isolated element must be zero,

From Figure 5.13 it can be observed that the bond stresses cancel each other; in consequence, the shear stress acting on the horizontal surface at the level of the steel reinforcement will only depend on the acting stresses on the FRP sheets caused by external loads. Therefore, the only unknown is the peak value σ_p, which is a principal stress, because there should be a constant ratio between the peak stresses for the tension (σ_p) and the compression zones. If this principal stress σ_p is larger than the modulus of rupture of concrete the failure will occur. Since the maximum peak σ_p must be located at the position shown in order to assure the equilibrium, it can be concluded that the horizontal crack develops towards the midspan. As was previously mentioned, the horizontal crack starts from any flexural crack between the cutoff point of the sheets and the maximum bending region.

The flexural crack spacing can be estimated from existing literature (Wang, Ling, 1998). At this point, the value of the maximum σ_p caused by the acting bending moment and shear force can be computed by equilibrium. More experimental and analytical work is needed to develop a numerically acceptable solution.

6. CONCLUSIONS AND FUTURE RESEARCH

6.1. CONCLUSIONS

Strengthening of RC beams with externally bonded CFRP sheets is effective and leads to increases in flexural strengthening between 30% to 60%. The following conclusions are drawn from the experimental and analytical phases carried out in this investigation:

6.1.1. Experimental Phase.

1. Premature failure in beams strengthened with CFRP sheets was observed, which was caused by concrete cover delamination. Two modes of failure within this failure were observed, which were called failure Mode I and failure Mode II in this investigation.

- Failure Mode I is caused by concrete cover delamination starting at the cutoff point of the laminate, which is originated by a high concentration of normal (out-of-plane) and shear stresses at that point. This mode of failure may occur when the laminate is relatively thick (i.e. when more than one ply of FRP is attached to the concrete surface).
- Failure Mode II is caused by cover delamination starting at an intermediate flexural crack, which is originated by splitting of concrete at the level of the steel reinforcement, and primarily, by normal (out-of-plane) and shear stresses at that level.

2. During each test, it was observed that the employment of CFRP sheets delayed the presence of the first visible cracks. Similarly, the flexural crack spacing was reduced when the number of plies of CFRP was increased. Also, the use of U-

jackets lessened the effect of the cover delamination failure by delaying the final failure.

3. The test results showed that by employing externally bonded sheets, important increases in flexural stiffness and ultimate capacity are achieved. However, these increases were afforded at the sake of some ductility losses.
4. Beams strengthened with the same amount of CFRP with different bonded areas had similar behavior.
5. Stirrup spacing did not have a significant influence on concrete cover delamination.

6.1.2.Analytical Phase. The mechanisms of the observed modes of failure are described. For Failure Mode I an analytical approach to estimate the shear and normal stresses at the curtailment of FRP sheets is presented. The values of the stresses can be expressed as a function of the shear force and bending moment at the cutoff point. By imposing that the principal tensile stress be less than the tensile strength of concrete, the safe values of the shear force and bending moment can then be derived.

The mechanism of Failure Mode II is complex. Schemes intending to predict the failure can be implemented. They can include the analysis of an element between two flexural cracks and the assumption of certain normal stress distribution similar to that employed for Mode I. This may serve as framework for future investigations.

6.2. RECOMMENDATIONS FOR FUTURE RESEARCH

Owing to the existing practices in the field, such as the number of sheets, thickness of laminate and tapering multiple sheets when required, Failure Mode II is more common. Therefore, analytical work is needed in order to obtain the magnitude of the normal and shear stresses that cause failure.

The effect of the bonded area needs to be addressed. By comparing beams strengthened with the same amount of FRP on different bonded areas, the influence of the stiffness (EA) of the laminate, if this is the case, would be determined.

By studying the effect of the total bonded length, it is expected to obtain Moment vs. Curvature curves with the same trend, only varying the moment at failure. In this way the influence of the total bonded length would be observed.

APPENDIX A

CRACKING PATTERN

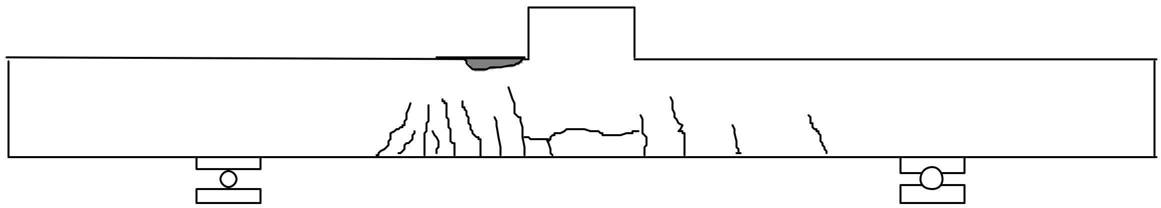

Figure A.1. Cracking Pattern – Beam CB

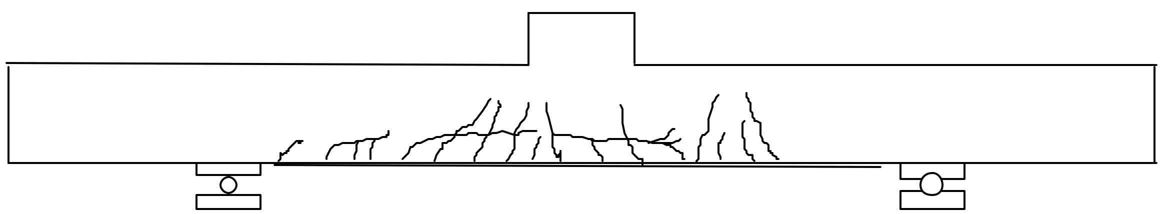

Figure A.2. Cracking Pattern – Beam B1P

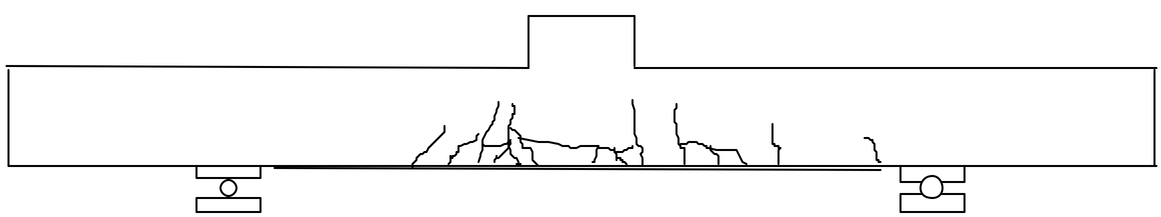

Figure A.3. Cracking Pattern – Beam B2P

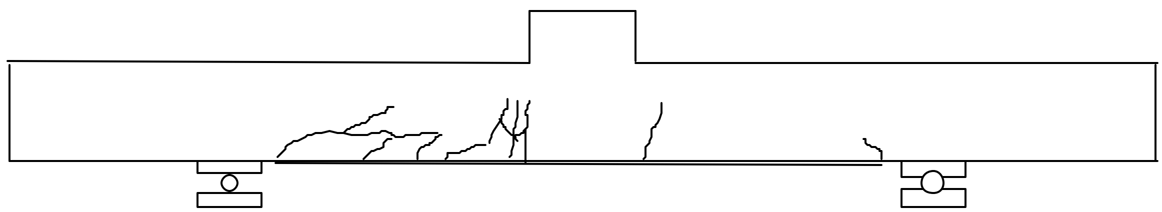

Figure A.4. Cracking Pattern – Beam B3P

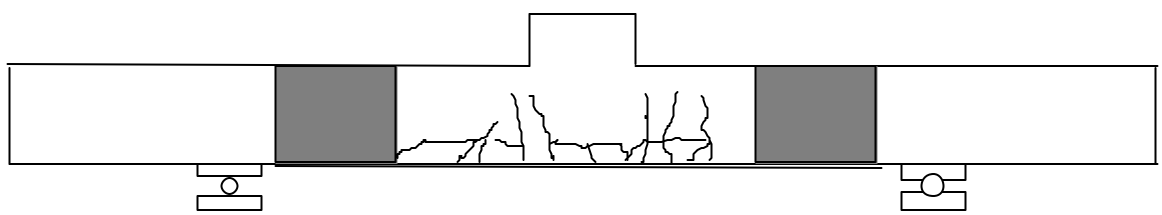

Figure A.5. Cracking Pattern – Beam B3PP

APPENDIX B

PHOTOGRAPHS OF TEST BEAMS

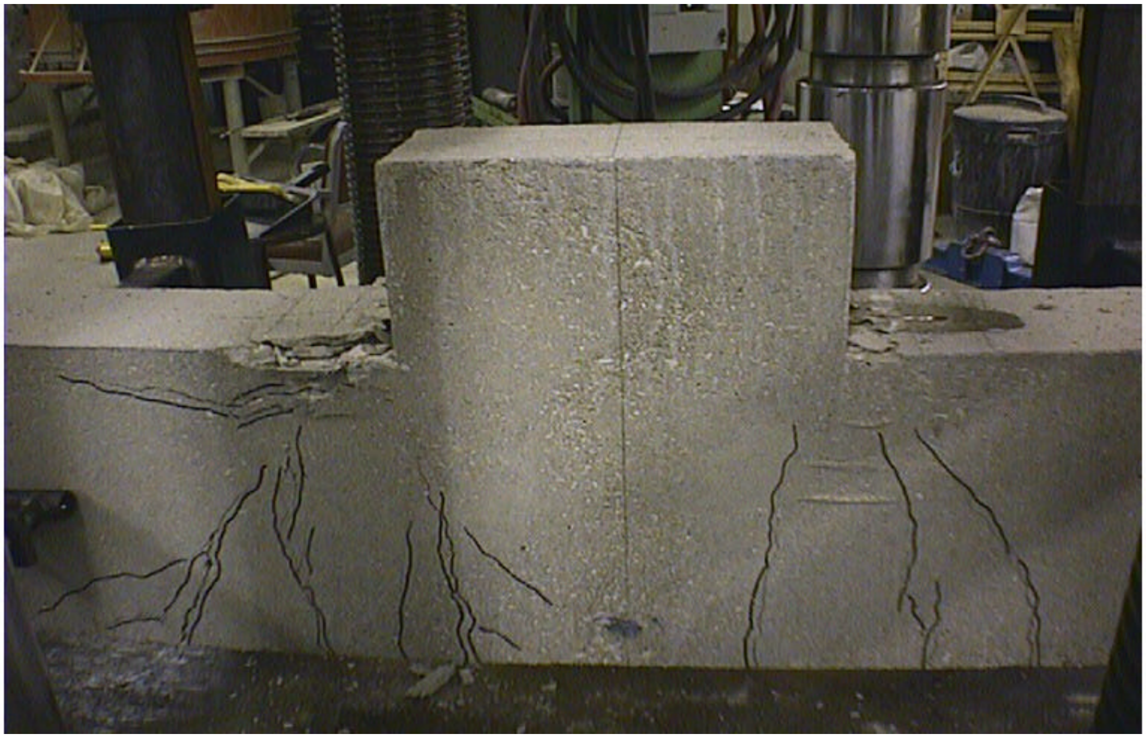

Figure B.1. Failure in Beam A0

Figure B.2. Failure in Beam A1

Figure B.3. Failure in Beam A3

Figure B.4. Failure in Beam A4

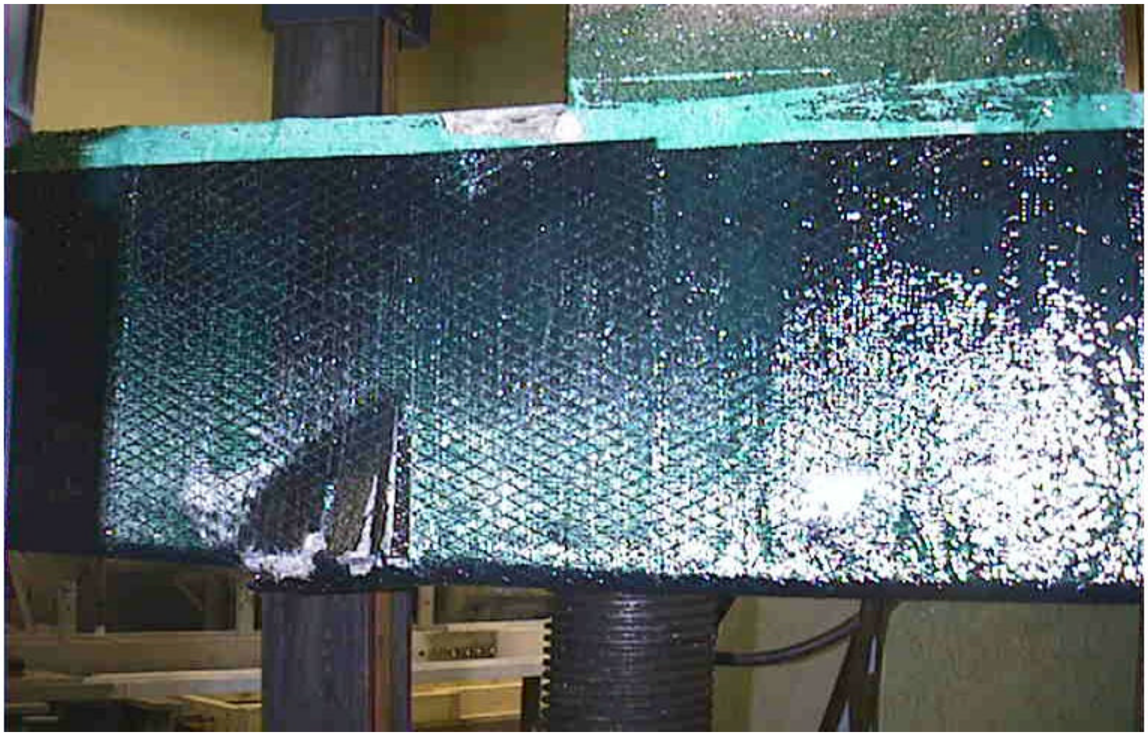

Figure B.5. Failure in Beam A5

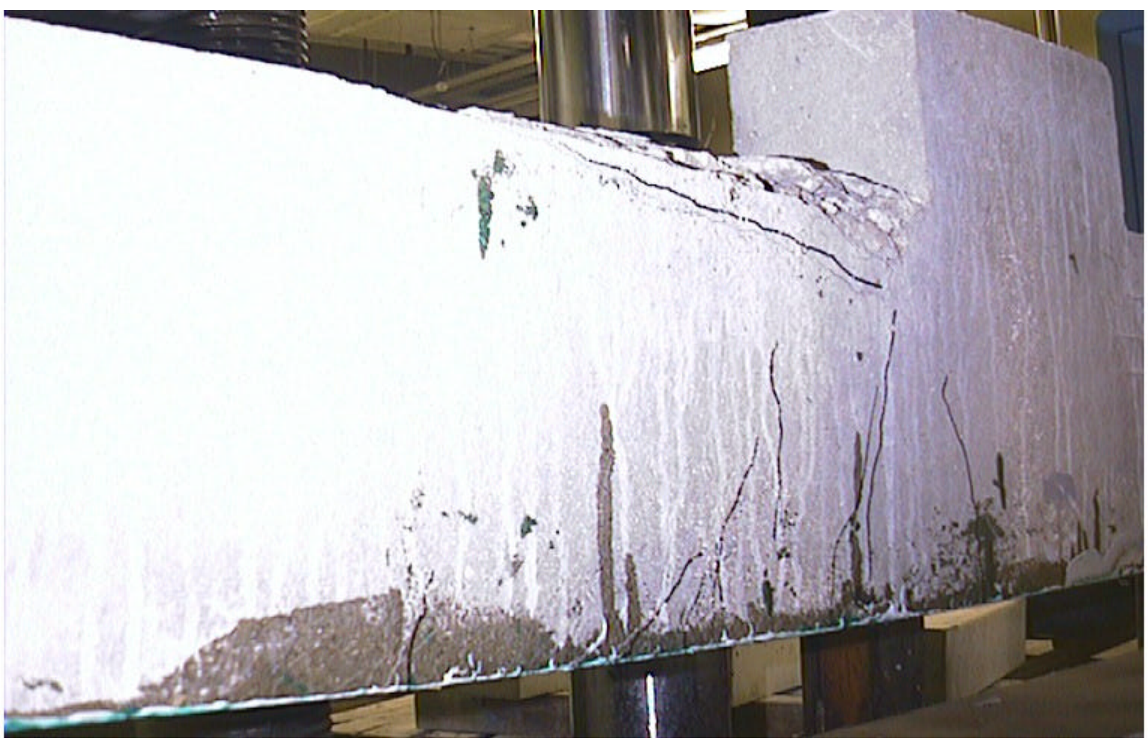

Figure B.6. Failure in Beam B0

Figure B.7. Failure in Beam B2

Figure B.8. Failure in Beam C1

APPENDIX C

CALCULATIONS PERTAINING TO COVER DELAMINATION FAILURE

EVALUATION OF MALEK MODEL

GEOMETRIC PROPERTIES

b=	6	in
h=	12	in
d=	10	in
ds=	2	in
d'=	2	in
As=	0.62	in^2
As'=	0.62	in^2

MATERIAL PROPERTIES

Concrete

f'c=	7500	psi
Ec=	4936	Ksi

Steel

fy=	62	psi
Es=	28300	Ksi

FRP

wf=	6	in
tf=	0.140	in
ta=	0.06	in
n=	3	plies
Ef=	33400	Ksi
Ea=	290	Ksi
υ=	0.36	
Ga=	107	Ksi

CROSS SECTIONAL PROPERTIES

ns=	5.73	
nf=	6.77	

	A	y	Ay	I	$(Y-y)^2$	$A(Y-y)^2$	$I+A(Y-y)^2$
1	72	6.06975	437.022	864	0.169343	12.19269	876.1927
2	2.934452	10.06975	29.5492	0	19.46145	57.10868	57.10868
3	2.934452	2.06975	6.073582	0	12.87724	37.78764	37.78764
4	5.663259	0	0	0	32.01565	181.3129	181.3129
	83.53216		472.6448				

y=	5.658	in
Itr=	1.15E+03	in^4
yc=	6	in
Ic=	8.64E+02	in^4
yf=	0.06975	in
If=	1.36E-03	in^4

SHEAR STRESS

P=	53.3	Kips	Ultimate Load (INPUT)
$M(x_o)$=	26.65	x_o	Kips x in
a1=	0		
a2=	26.65		
a3=	0		
Lo=	5	in	Distance between origin of x_o and cutoff point
A=	0.38138		
b1=	0.0000		
b2=	0.8854		
b3=	4.427		
C1=	4.427		
C2=	-4.427		

t(x)= 0.381 cosh (0.618 x) -0.381 sinh (0.618 x) + 0.000 x + 0.124

tmax= 0.505 Ksi

TENSILE STRESS IN THE FRP SHEET

fp(x)= 4.427 sinh (0.618 x) -4.427 sinh (0.618 x) + 0.000 x^2 + 0.885 x + 4.427

NORMAL (PEELING) STRESS

q=	0	K/in	Distributed load
Kn=	4833.3	Ksi/in	
β=	3.5561	in^{-1}	
Vc=	8.475	Kips	
Vp=	-0.211	Kips	
Mo=	133.250	Kips x in	Bending moment in the concrete beam at the plate end due to externally applied load
D1=	-0.25653	Ksi	
D2=	0.00597	Ksi	

fn(x)= $e^{-3.556\,x}$ [-0.257 cos(3.556 x) + 0.006 sin(3.556 x)]

EVALUATION OF ROBERTS MODEL

GEOMETRIC PROPERTIES

b=	6	in
h=	12	in
d=	10	in
ds=	2	in
As=	0.62	in^2
As'=	0.62	in^2

MATERIAL PROPERTIES

Concrete

f'c=	7500	psi
Ec=	4936	Ksi

Steel

fy=	62	psi
Es=	28300	Ksi

FRP

wf=	6	in
tf=	0.140	in
ta=	0.06	in
n=	3	plies
Ef=	33400	Ksi
Ea=	290	Ksi
υ=	0.36	
Ga=	107	Ksi
ns=	5.73	
nf=	6.77	

CALCULATIONS

	A	h	A.h	$(h-x)^2$	I	$A.(h-x)^2$	$I+A.(h-x)^2$
1	72.000	6.07	437.02	0.17	864.00	12.19	876.19
2	2.934	10.07	29.55	19.46	0	57.11	57.11
3	2.934	2.07	6.07	12.88	0	37.79	37.79
4	5.663	0.00	0.00	32.02	0	181.31	181.31
	83.532		472.64				

y=	5.66	in
I=	1152.40	in^4

CALCULATIONS

P=	53.3	Kips	Ultimate Load
Lo=	5	in	
V=	26.65	Kips	
M=	133.25	Kipsxin	
t_{max}=	**0.505**	**Ksi**	
fn_{max}=	**0.257**	**Ksi**	

PRINCIPAL STRESS

σ= 0.649 Ksi **$7.50\,(f'c)^{0.5}$**

L=	7	ft
a=	79	
t_{10}=	0.548	
t_{1a}=	0.548	
τ_1=	0.124	
Ks=	10661.8	

$\tau_2(x)$= 0.696 (-0.548 sinh 0.618 x + 0.548 cosh 0.618 x)

α^2= 0.381

$t(x)$= -0.381 sinh (0.618 x) + 0.381 cosh (0.618 x) + 0.124

Eplp/Eplp+Eclc=	1.063E-05
f_{20}=	0.212
m_{20}=	0.00142
γ^4=	159.92

$s(x)$= $e^{-3.556x}$ [0.257 cos (3.556 x) - 0.006 sin (3.556 x)]

CALCULATION OF SHEAR AND NORMAL STRESSES AT FAILURE
1 PLY OF CFRP

GEOMETRIC PROPERTIES

b=	6	in
h=	12	in
d=	10	in
ds=	2	in
As=	0.62	in^2
As'=	0.62	in^2

MATERIAL PROPERTIES

Concrete

f'c=	7500	psi
Ec=	4936	Ksi

Steel

fy=	62	psi
Es=	28300	Ksi

FRP

wf=	6	in	
tf=	0.047	in	
ta=	0.06	in	*primer+putty+1st.layer of epoxy*
n=	1	plies	
Ef=	33400	Ksi	
Ea=	290	Ksi	
υ=	0.36		
Ga=	107	Ksi	
ns=	5.73		
nf=	6.77		

CALCULATION OF CENTROID AND MOMENT OF INERTIA

	A	h	A.h	$(h-x)^2$	I	$A.(h-x)^2$	$I+A.(h-x)^2$
1	72.000	6.02	433.67	0.02	864.00	1.46	865.46
2	2.934	10.02	29.41	17.16	0	50.36	50.36
3	2.934	2.02	5.94	14.88	0	43.66	43.66
4	1.888	0.00	0.00	34.58	0	65.28	65.28

h=	5.88	in
I=	1024.77	in^4

CALCULATION OF NORMAL AND SHEAR STRESSES

P=	43.4	Kips	Ultimate Load
Lo=	5	in	
V=	21.7	Kips	
M=	108.50	Kipsxin	
t **=**	0.249	Ksi	
s_y**=**	0.094	Ksi	
s_x**=**	0.623	Ksi	

PRINCIPAL STRESS

s **=**	0.721	Ksi	**8.33 $(f'c)^{0.5}$**
q =	21.6	^{o}	

CALCULATION OF SHEAR AND NORMAL STRESSES
2 PLIES OF CFRP

GEOMETRIC PROPERTIES

b=	6	in
h=	12	in
d=	10	in
ds=	2	in
As=	0.62	in^2
As'=	0.62	in^2

MATERIAL PROPERTIES

Concrete

f'c=	7500	psi
Ec=	4936	Ksi

Steel

fy=	62	psi
Es=	28300	Ksi

FRP

wf=	6	in	
tf=	0.093	in	
ta=	0.06	in	*primer+putty+1st.layer of epoxy*
n=	2	plies	
Ef=	33400	Ksi	
Ea=	290	Ksi	
υ=	0.36		
Ga=	107	Ksi	
ns=	5.73		
nf=	6.77		

CALCULATION OF CENTROID AND MOMENT OF INERTIA

	A	h	A.h	$(h-x)^2$	I	$A.(h-x)^2$	$I+A.(h-x)^2$
1	72.000	6.05	435.35	0.08	864.00	5.63	869.63
2	2.934	10.05	29.48	18.32	0	53.74	53.74
3	2.934	2.05	6.01	13.84	0	40.62	40.62
4	3.776	0.00	0.00	33.26	0	125.56	125.56

h=	5.77	in
I=	1089.55	in^4

CALCULATION OF NORMAL AND SHEAR STRESSES

P=	40.7	Kips	Ultimate Load
Lo=	5	in	
V=	20.35	Kips	
M=	101.75	Kipsxin	
τ=	0.324	Ksi	
σ_y=	0.145	Ksi	
σ_x=	0.539	Ksi	

PRINCIPAL STRESS

σ =	0.721	Ksi	**8.33 $(f'c)^{0.5}$**
θ =	29.4	^{o}	

CALCULATION OF SHEAR AND NORMAL STRESSES
3 PLIES OF CFRP

GEOMETRIC PROPERTIES

b=	6	in
h=	12	in
d=	10	in
ds=	2	in
As=	0.62	in^2
As'=	0.62	in^2

MATERIAL PROPERTIES

Concrete

f'c=	7500	psi
Ec=	4936	Ksi

Steel

fy=	62	psi
Es=	28300	Ksi

FRP

wf=	6	in	
tf=	0.140	in	
ta=	0.06	in	*primer+putty+1st.layer of epoxy*
n=	3	plies	
Ef=	33400	Ksi	
Ea=	290	Ksi	
υ=	0.36		
Ga=	107	Ksi	
ns=	5.73		
nf=	6.77		

CALCULATION OF CENTROID AND MOMENT OF INERTIA

	A	h	A.h	$(h-x)^2$	I	$A.(h-x)^2$	$I+A.(h-x)^2$
1	72.000	6.07	437.02	0.17	864.00	12.19	876.19
2	2.934	10.07	29.55	19.46	0	57.11	57.11
3	2.934	2.07	6.07	12.88	0	37.79	37.79
4	5.663	0.00	0.00	32.02	0	181.31	181.31

h=	5.66	in
I=	1152.40	in^4

CALCULATION OF NORMAL AND SHEAR STRESSES

P=	38.6	Kips	Ultimate Load
Lo=	5	in	
V=	19.3	Kips	
M=	96.50	Kipsxin	
t **=**	0.366	Ksi	
s_y**=**	0.181	Ksi	
s_x**=**	0.474	Ksi	

PRINCIPAL STRESS

s **=**	0.721	Ksi	**8.33 $(f'c)^{0.5}$**
q =	34.1	^{o}	

CALCULATION OF SHEAR AND NORMAL STRESSES
4 PLIES OF CFRP

GEOMETRIC PROPERTIES

b=	6	in
h=	12	in
d=	10	in
ds=	2	in
As=	0.62	in^2
As'=	0.62	in^2

MATERIAL PROPERTIES

Concrete

f'c=	7500	psi
Ec=	4936	Ksi

Steel

fy=	62	psi
Es=	28300	Ksi

FRP

wf=	6	in	
tf=	0.186	in	
ta=	0.06	in	*primer+putty+1st.layer of epoxy*
n=	4	plies	
Ef=	33400	Ksi	
Ea=	290	Ksi	
υ=	0.36		
Ga=	107	Ksi	
ns=	5.73		
nf=	6.77		

CALCULATION OF CENTROID AND MOMENT OF INERTIA

	A	h	A.h	$(h-x)^2$	I	$A.(h-x)^2$	$I+A.(h-x)^2$
1	72.000	6.09	438.70	0.29	864.00	20.89	884.89
2	2.934	10.09	29.62	20.60	0	60.45	60.45
3	2.934	2.09	6.14	11.98	0	35.16	35.16
4	7.551	0.00	0.00	30.85	0	232.96	232.96

h=	5.55	in
I=	1213.45	in^4

CALCULATION OF NORMAL AND SHEAR STRESSES

P=	36.95	Kips	Ultimate Load
Lo=	5	in	
V=	18.475	Kips	
M=	92.38	Kipsxin	
t =	0.391	Ksi	
s_y=	0.208	Ksi	
s_x=	0.423	Ksi	

PRINCIPAL STRESS

s =	0.721	Ksi	**8.33 $(f'c)^{0.5}$**
q =	37.3	^{o}	

BIBLIOGRAPHY

ACI-318-95, (1995), "Building Code Requirements for Reinforced Concrete and Commentary," American Concrete Institute, Detroit Michigan.

An, W., Saadatmanesh, H., and Ehsani, M. R., (1991), "RC Beams Strengthened with FRP Plates, II: Analysis and Parametric Study," Journal of Structural Engineering, American Society of Civil Engineers, Vol. 117, No. 11, November, 1991, pp. 3434-3455.

Arduini, A., Di Tommaso, A., and Manfroni, O., (1995), "Fracture Mechanisms of Concrete Beams Bonded with Composite Plates," Non-metallic (FRP) Reinforcements for Concrete Structures, E&FN, London, 1995, pp. 484-491.

Bazant, Z., and Oh, B., (1984), "Deformation of Progressively Cracking Reinforced Concrete Beams," American Concrete Institute Journal, May-June 1984, pp. 268-278.

Blaschko, M., Niedermeier, R., and Zilch, K., (1998), "Bond Failure Modes of Flexural Members Strengthened with FRP," Second International Conference on Composites in Infrastructures", Tucson, Arizona, 1998, pp. 450-461.

Chaallal, O., Nollet, M. J., and Saleh, S., (1998), "Use of CFRP Strips for Flexure and Shear Strengthening of RC Members," Second International Conference on Composites in Infrastructures, Tucson, Arizona, 1998, pp. 249-260.

Chajes, M.J., Thomson, T. A., Jr., and Tarantino, B., (1995), "Reinforcement of Concrete Structures Using Externally Bonded Composite Materials," Non-metallic (FRP) Reinforcements for Concrete Structures, E&FN, London, 1995, pp. 501-508.

Deshmukh, V., (1995), "Ultimate Behavior of Reinforced Concrete Beams Externally Bonded with FRP Laminates," Thesis in Architectural Engineering, The Pennsyvania State University, 1995.

He, J. H., Pilakoutas, K., and Waldron, P., (1997), "Strengthening of Reinforced Concrete Beams with CFRP Plates," Proceedings of the Third International Symposium on Non-metallic (FRP) Reinforcements for Concrete Structures, Vol. 1, October, 1997, pp. 343-350.

Jones, R., Swamy, R. N., and Charif, A., (1988),"Plate Separation and Anchorage of Reinforced Concrete Beams Strengthened with Epoxy-Bonded Steel Plates," The Structural Engineer, Vol. 66, No. 5, March, 1988, pp. 85-94.

MacGregor, J., (1997), Reinforced Concrete Mechanics and Design, Prentice-Hall Inc., Upper Saddle River, New Jersey.

Maeda, T., Asano, Y., Sato, Y., Ueda, T., and Kakuta, Y., (1997), "A Study on Bond Mechanism of Carbon Fiber Sheet," Proceedings of the Third International Symposium on Non-metallic (FRP) Reinforcements for Concrete Structures, Vol. 1, October, 1997, pp. 279-286.

Malek, A., Saadatmanesh, H, and Ehsani, M.R., (1998), "Prediction of Failure Load of R/C Beams Strengthened with FRP Plate Due to Stress Concentration at the Plate End," Structural Journal, American Concrete Institute, Vol. 95, No. 1, March-April, 1998, pp. 142-152.

M'Bazaa, I., Missihoun, M., and Labossiere, P., (1996), "Strengthening of Reinforced Concrete Beams with CFRP Sheets," First International Conference on Composites in Infrastructure Fiber, ICCI'96, Tucson, Arizona, pp. 746-759.

Mirza, S., Hatzinikolas, M., and MacGregor, J., (1979), "Statistical Descriptions of the Strength of Concrete," Journal of Structural Engineering, American Society of Civil Engineers, Vol. 105, No.516, June, 1979, pp. 1021-1037.

Nanni, A., Di Tomasso, A., and Arduini, M., (1997), "Behavior of RC Beams Strengthened with Carbon FRP Sheets," Research Report Part II: Continuous Beams, University of Bologna, Italy, March, 1997, pp.1-16.

Oehlers, D. J. and Moran, J. P., (1990). "Premature Failure of Externally Plated Reinforced Concrete Beams," Journal of Structural Engineering, American Society of Civil Engineers, Vol. 116, No. 4, April 1990, pp. 978-995.

Roberts, T. M., (1989), "Approximate Analysis of Shear and Normal Stress Concentrations in the Adhesive Layer of Plated RC Beams," The Structural Engineer, Vol. 67, No. 12, June, 1989, pp.224-233.

Saadatmanesh, H., and Ehsani, M.R., (1991), "RC Beams Strengthened with GFRP Plates, I: Experimental Study," Journal of Structural Engineering, American Society of Civil Engineers, Vol. 117, No. 11, November, 1991, pp. 3417-3433.

Serra, P., (1996), "Stato Coattivo con Fasce di Composito per il Reinforzo di Travi in Conglomerato Cementizio Armatu Fessurate," Thesis in Civil Engineering, The University of Bologna, Italy, 1996.

Takahashi, Y., Sato, Y., Ueda, T., Maeda, T., and Kobayashi, A., (1997), "Flexural Behavior of RC Beams with Externally Bonded Carbon Fiber Sheet," Proceedings of the Third International Symposium on Non-metallic (FRP) Reinforcements for Concrete Structures, Vol. 1, October, 1997, pp. 327-334.

Taljsten, B., (1997), "Strengthening of Beams by Plate Bonding," Journal of Materials in Civil Engineering, Vol. 9, No. 4., November, 1997, pp. 206-212.

Tumialan, J. G., (1998), “Concrete Cover Delamination in Reinforced Concrete Beams Strengthened with CFRP Sheets,” MSc Thesis Department of Civil Engineering, The University of Missouri, Rolla, MO.

Wang, C., Ling, F., (1998), “Prediction Model for the Debonding Failure of Cracked RC Beams with Externally Bonded FRP Sheets,” Second International Conference on Composites in Infrastructure, Tucson, Arizona, 1998, pp 548-562

Zhang, S., Raoof, M., and Wood, L. A. (1995), “Prediction of Peeling Failure of Reinforced Concrete Beams with Externally Bonded Steel Plates,” Proceedings of the Institution of Civil Engineers, Structures and Buildings, August, 1995, pp. 257-268.